Triumph Motorcycle Engine Performance Tuning and Engine Dynamometer Development

Written by Seth N. DeValve under the direction of Prof. Michael G. Littman
Class of 2016

Submitted to the
Department of Mechanical and Aerospace Engineering
Princeton University
In partial fulfillment of the requirements
Of Undergraduate Independent Work/Senior Thesis

Final Report
January 5th, 2016

Advisor: Professor Michael G. Littman
Reader: Professor Daniel M. Nosenchuck
MAE 339 and 339D
74 Pages
Advisor's copy

Acknowledgements

Thank you Dad, Mom, Caleb, Levi, and Jacob, for your tremendous examples in my life. You are all responsible for any success I have had.

Thank you Professor Littman, for not only your thoughtful oversight of my senior thesis project, but also of my independent work over the last 3 years.

Thank you Jon Prevost, for spending afternoons getting your hands dirty with me, for staying after hours, for all of your technical input, and for being a great friend.

Thank you Glenn Northey, for your instruction in the machine shop and teaching to me to be a capable and independent machinist.

Table of Contents

List of Figures

List of Terms

Dyno: Short for Dynamometer**.** Test bed which measures engine metrics over its entire rpm range

PAU: Power Absorption Unit. Unit which provides load to the engine output gear.

No load speed: An engine's max rpm when no additional load is applied.

Engine Stall: The condition when an engine's rpm drops to zero due to an immovable load.

Dynamic Filter: A signal averager which uses an external clock to determine sample size.

Static Filter: A signal averager which uses an internal clock to determine sample size.

Manifold: The ducting that serves as the funnel for aspirated air into the intake valve or out of the exhaust valve.

Eddy Current: A current which is induced in a conductive material when in the presence of a changing magnetic field. The magnetic polarity of the eddy current is opposite that of the polarity of the magnetic field that induced it.

Faraday's Law: The induced electromotive force in any closed circuit is equal to the negative of the time rate of change of the magnetic flux enclosed by the circuit.

Lenz's Law: An induced electromotive force always gives rise to a current whose magnetic field opposes the original change in magnetic flux.

Abstract

This paper presents the progress of data acquisition quality from the MAE department's engine dynamometer and provides initial verification of the fidelity of the data acquired. Verification is achieved by way of presenting DC motor torque curves measured on the dyno which agree with the theoretical framework from electromagnetic theory. Further verification is achieved by way of presentation of dyno data measured from a 1956, single cylinder, 200cc, Triumph motorcycle engine and comparison with engine modeling software and the 1956 published curve. The results presented reveal a very good agreement between the empirical, numerical, and 1956 published curve which grants reliability to the engine dynamometer as well as validity to the engine modeling software. Further validity is given to the torque curves through a qualitative and quantitative study on engine resonance. Lastly, additional improvements are suggested to continue to improve the data acquisition quality, as well as recommendations for future research.

Introduction

The use of dynamometers (dyno for short) in transportation performance testing is nothing new. In fact the earliest recorded invention and use of a dyno dates back to 1828 when Gaspard de Prony invented de Prony Brake, an early dyno model that operated by applying increasing friction to an engine's output drum.[i] This design was further developed by Charles Babbage in 1838, who, better known as the father of the computer, introduced a dynamometer car to measure the pulling power of English railroad locomotives.[ii] Almost a century later, the type of dyno used in the experiments in this paper, an eddy current Power Absorption Unit dyno, was first invented in 1931 by Martin and Anthony Winther.[iii]

The concept of how a dynamometer works is simple. A dynamometer is any device that can provide variable and continuous load to an object that produces continuous power. In modern times, the power producer is usually some sort of engine, either on its own or connected in its power train. The variable load is created by the power absorption unit (PAU for short). Many different forms of PAU's exist and are used. Hydraulic PAU's use viscous effects in water to absorb power from an engine, inertial dyno's utilize a very heavy flywheel to accomplish the same thing, and eddy current dynos absorb power by spinning a conductive rotor in the presence of a magnetic field.

History

In earlier days however, people were more concerned with the power of their horses than the power of their cars. Instead of engines and magnetic brakes they used horses and a stack of weights. Because horses were the primary laborers in farming and transportation, people sought ways to test the strength of their horses and pit them against each other. In 1923, the draft horse dyno was invented for just this very purpose.[iv] A draft horse dyno is a series of weights and harnesses which are stretched out across a field, each successive load being heavier than the previous. The competition is composed of a horse, which is first hitched into the lightest harness, and proceeds to pull it across the soil. As long as the horse is successful in pulling the weight, it continues down the line of heavier weights until it can no longer pull the weight a short distance. In this way, a farmer knows how strong his horse is and how it compares to his neighbor's horse. Such a competition is still practiced and is the basis for the Eastern Draft Horse Association, the largest horse pulling organization in the United States.[v] While much more primitive than the dynamometer used in this paper, the draft horse dyno represents the basic concepts of how an engine dynamometer works. A power producer, in this case a horse, is capable of only a finite level of power output, which is measured by an ever increasing load. In the absence of any load, a horse is free to run as fast as it can. This is called the power producer's *no load speed.* However the horse can only run so fast with load attached to its back, and eventually it will no longer be able to move. In an engine this is called *engine stall*. At this point in time a measurement can be taken to determine how strong the horse is. This is the horse's maximum strength. Because an

engine produces power through a rotating crankshaft, the analogous parameter is called *max torque*.

The horse represents a linear system from a measurement perspective. A linear force producer is one where the output force is related to its speed by a constant value. Like an electric motor, a horse's minimum applied force occurs at its no load speed and its maximum applied force occurs at stall. However for an internal combustion engine, maximum torque does not occur at engine stall and the path connecting the torque values at engine stall and no-load speed is highly nonlinear.

Unfortunately the draft horse dyno has limited scientific explanatory power. The test can only tell you the horse's maximum pulling force (and only because it is a linear system). It cannot tell a farmer which horse is most powerful. Power is work (or torque) multiplied by speed. In order to measure a horse's power, its pulling force, distance traveled, and time elapsed all need to be measured. Yet still, the question of finding the horse's *maximum* power remains problematic. This is where modern data acquisition equipment comes in handy. A modern dynamometer only uses two transducers – an rpm transducer and a force transducer. With these two measurements, torque and power over the engine's entire rpm range can be derived. Such data acquisition allows an engineer to know the maximum power of an engine and at what rpm it occurs, as well as the maximum torque and its associated rpm for both linear and nonlinear systems.

Experimental Setup and Theoretical Framework

The dynamometer used for the studies in this thesis is a universal engine dynamometer. It is universal in the sense that it can both drive and be driven. It is also considered an engine dyno

Figure 1: Engine Dynamometer schematic. The variable reluctance rpm sensor turns magnetic pulses into a digital square wave, whose rising edges are counted in the DAQ system and converted to dyno rpm.

as opposed to a chassis dyno because the engines tested are decoupled from their chassis' and

mounted separately onto the dyno frame. The driver is an AC motor which is coupled to the PAU through a compressed air-actuated solenoid clutch. In IC engine experiments, the AC motor serves as a starter motor. The PAU is an eddy current brake. An eddy current brake is a series of electromagnets which act as stators surrounding a rotating conductive flywheel. An eddy current, in the electrical sense, is a circular electrical current that results in the conductor when the conductor encounters a changing magnetic field. An eddy current in electronics is analogous to eddy currents in fluid dynamics, where circular currents may result in a fluid when the fluid encounters a symmetric pressure differential.

In fluid dynamics, a ball thrown through the air is analogous to a steel rotor spinning in the presence of a magnetic field. The thrown object is like the steel rotor on the eddy current brake. Air molecules are like the magnetic field. When an object gets thrown through the air, it disturbs the surrounding air by making a pressure differential between the stagnation point on the front half of the object and the wake on the balk half. Because fluid flows from high pressure to low pressure, air on the periphery of the wake wants to flow into the low pressure area in the wake on all sides, causing this air to circle upstream. These air currents rotate in a circle, and are given the name eddy currents (see Figure 2). The inclination of an eddy current to flow upstream is a natural scientific law which in analog electronics is described by *Lenz's Law.* The fluid dynamics analogue of Lenz's law states that the direction of the induced air current (in this case, the eddy current caused by a pressure differential) is such that it attempts to undo the change in the surrounding air. Therefore the fluid surrounding the wake of a moving object swirls into the voided space in an attempt to undo the creation of the wake.

Pressure is just a manifestation of potential energy. Thus, just as a fluid flows from a region of high potential energy to a region of low potential energy, electrical current flows from an area of high potential energy to an area of low potential energy. In electronics, this potential energy is called a voltage. As a conductive rotor spins through electromagnets in the PAU, it is disturbing the magnetic field which causes a voltage differential, just as a ball disturbing the air produces a pressure differential. Faraday's Law predicts such behavior.
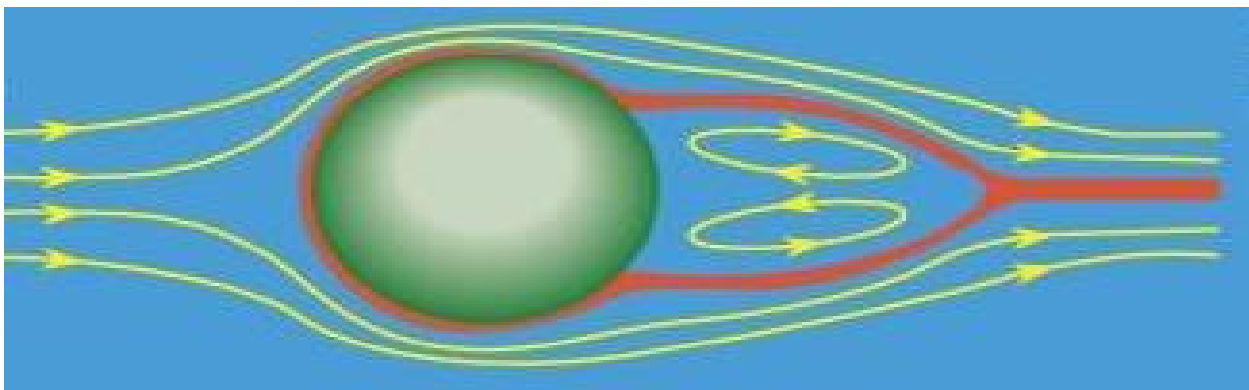
Figure 2: Eddy Currents forming in the wake of a thrown object

Faraday's Law states that any change in the magnetic environment of the rotor will cause a voltage to be induced in the conductor (steel rotor). The presence of a voltage causes current to flow toward the area of low potential, naturally causing a circular current acting in the direction that would undo the change in magnetic field according to Lenz's Law.

Lenz's Law: "An induced electromotive force always gives rise to a current whose magnetic field opposes the original change in magnetic flux."

Lenz's Law states that when an EMF is generated in the rotor by a change in magnetic flux due to Faraday's Law, the polarity of the induced EMF is such that it produces a current whose magnetic field opposes the change which produced it. It is the opposition of these two magnetic fields that creates the braking power in an eddy current PAU. In summary, the

Torque Measurement
(Power Absorption Unit)
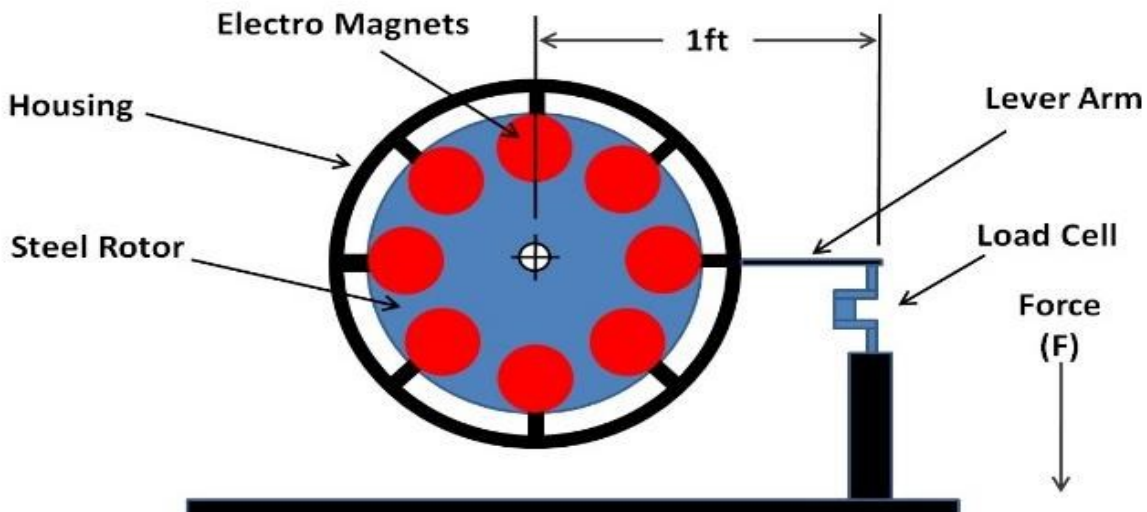
Figure 3: Power Absorption Unit. The brake housing is free to spin about its axis, only being restrained by the lever arm attached to the load cell. The load cell measures pound force, and the lever arm being exactly 1 foot off axis allows torque in units of ft-lbs to be directly measured

conductive rotor spins freely when the electromagnets are drawing no voltage. As the electromagnets begin to draw voltage, the rotor experiences a changing magnetic field as it spins. The changing magnetic field induces a voltage in the rotor which creates eddy currents throughout. The magnetic field produced by the eddy currents opposes the magnetic field in the electromagnets and slow the rotor to a stop. (Note that this process is purely

electrical, meaning if the rotor is not an electrical conductor, an eddy current cannot be formed).

Just as the pressure differential between the front and back half of an object thrown through the air is dependent on how fast the object is thrown, the braking force resulting from an eddy current is dependent on how fast the conductive rotor is spinning. Therefore if the rotor is not spinning, there is no brake force, even if the electromagnets are drawing maximum voltage. This is because there is no opposing magnetic field. However as the rotor spins faster, it encounters an ever increasing brake force. The strength of an eddy current is given by the formula:

$$I = -\frac{1}{R} * \frac{dB}{dt}$$
(EQ 1)

Where I is current, R is the resistance in the conductive material, and B is the strength of the magnetic field. Therefore the strength of the eddy current is proportional to the time rate of change in the magnetic field strength. Thus applying an increasing voltage to a conductive rotor will cause it to spin slower until the rotor stops completely. By the same principle, spinning the rotor faster in a constant magnetic field will produce an increasing braking force due to Lenz's Law. These two concepts represent the two methods in which dynamometer data can be taken:

Constant Force
"Constant Force" data is taken by setting the voltage of the eddy current brake and leaving it constant, while the speed of the rotor is varied throughout the operable range of the engine. "Constant Force" is put in quotes because the force measured is actually changing. The name of this data acquisition type is commonly used in dynamometer research for tests that involve a fixed setting on the PAU.

Constant Speed
"Constant Speed" data is gathered when a speed controller is available to keep the "speed of the engine constant". I put "constant speed" in quotation marks here because this is the type of test where you bring the engine from it's no load speed all the way to stall (speed is actually varying as well). It is called a "constant speed" test because what is manually varied is the braking force. In the case of an electric motor, the voltage given to the motor remains constant. In the case of a carbureted IC engine, the throttle position is held constant. In both cases the voltage given to the coils on the eddy current brake is slowly increased until engine stall is reached. **Unless otherwise noted, all of the data presented in this thesis are Constant Speed data.** There is are compromises and advantages for each type of test in the quality of data that is acquired, the specifics of which are detailed in Chapter 1.

Figure 4: Engine Dynamometer setup with the Triumph motorcycle engine, stands coupled
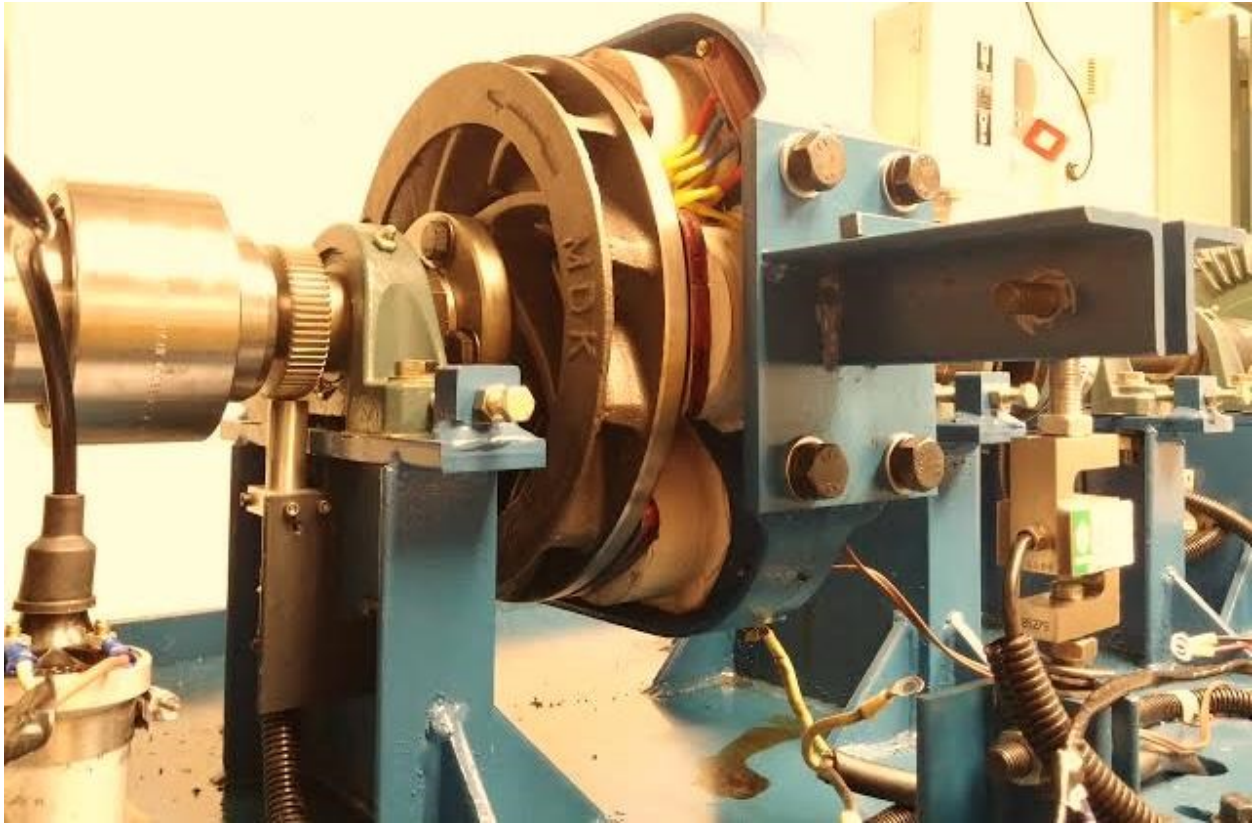
Figure 5: Close up of the Eddy Current brake and Data Acquisition equipment. Electrical coils can be seen on backside of steel rotor. Variable reluctance RPM sensor can be seen at left and Load Cell at right

Chapter 1: Dyno Calibration

Electric Motors are Linear Systems

It was noted in the introduction that a DC electric motor represents a linear system. This means that its minimum torque occurs at no load speed and its maximum torque occurs at engine stall, and all points in between connect in a straight line. This fact can be qualitatively shown through an understanding of back emf: Since the armature windings of a dc motor are moving through a magnetic field, they have a voltage induced in them. This voltage opposes the motor supply voltage and so is called "back electromotive force (emf)". The voltage is proportional to the running speed of the motor. The back emf of the motor, plus the voltage drop across the winding internal resistance and brushes, must equal the voltage at the brushes. This provides the fundamental mechanism of speed regulation in a DC motor. If the mechanical load increases, the motor slows down; a lower back emf results, and more current is drawn from the supply. This increased current provides the additional torque to balance the new load.[vii]

The linear response of a DC motor is very useful because it can be used for dyno calibration. If empirical data can be gathered that matches the relationship we would expect from electromagnetic theory, then we can be confident that the dynamometer will be capable of correctly analyzing nonlinear motor systems such as an internal combustion engines as well.

Two DC electric motors were employed for the task of calibrating the dynamometer. A Leeson 2HP DC electric motor and a Polyspede ½HP DC electric motor.

Figure 6: Leeson 2 HP DC motor at left and Polyspede 1/2 HP DC motor at right

As a reminder, a perfect dyno calibration would produce DC motor data that has a linear Torque vs RPM curve and a quadratic Power vs RPM curve, with maximum power occurring halfway between no load speed and engine stall. The data that follows are the results of the DC motor calibration tests.
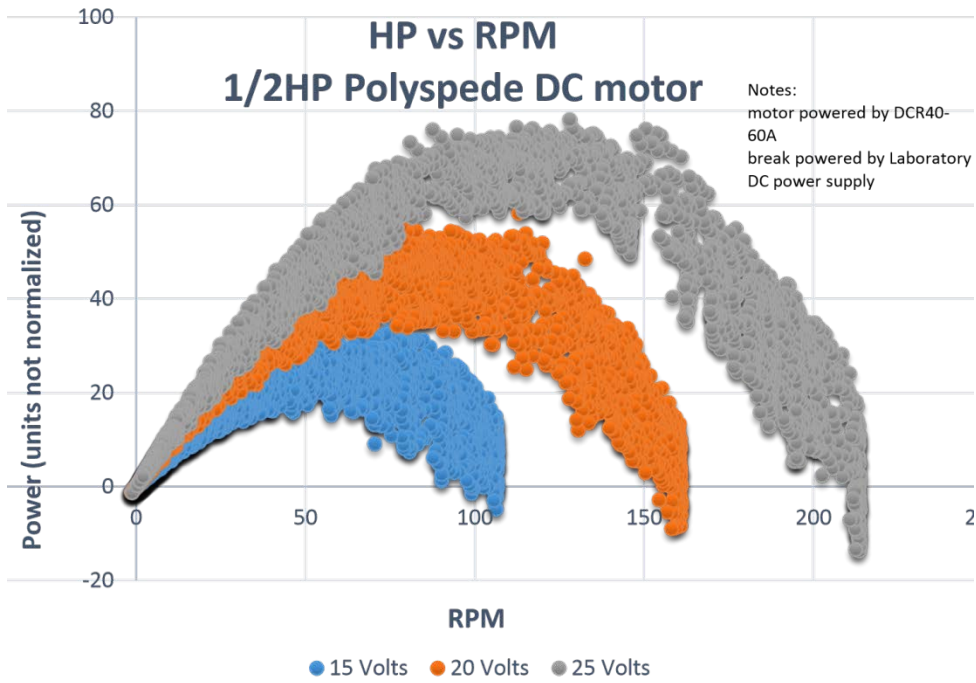
Figure 7: HP vs RPM data for 1/2 HP DC motor

Data
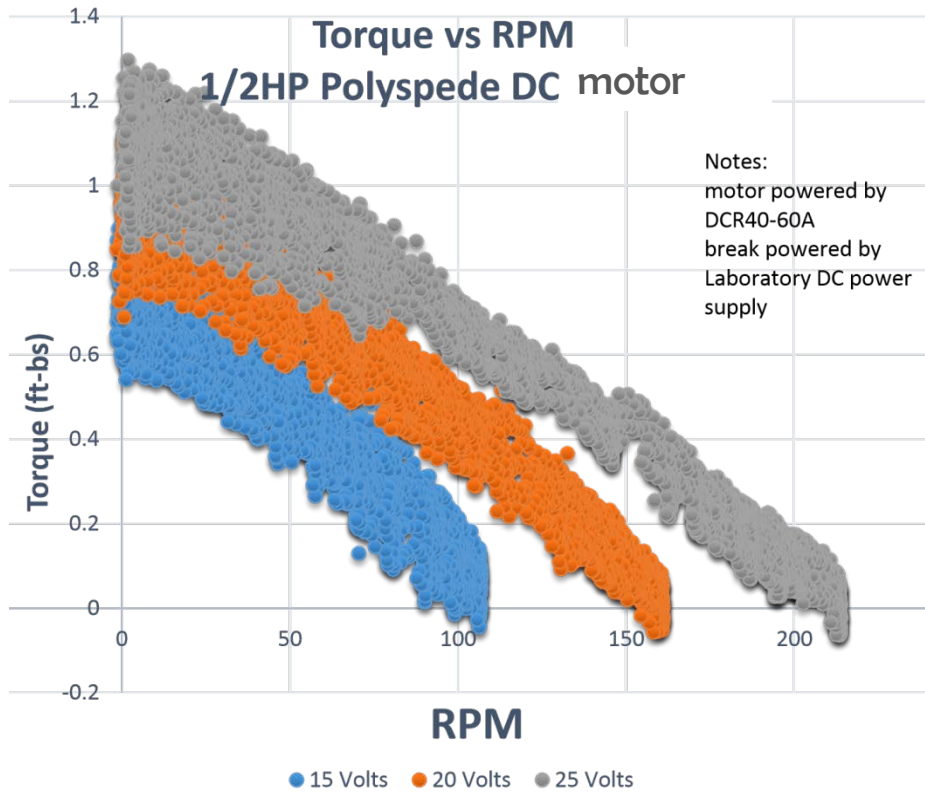
Figure 8: Torque vs RPM data for 1/2 HP DC motor

The ½HP DC motor tests proved to be a good start toward dynamometer calibration. The expected trend of a linear torque curve and a parabolic HP curve were achieved. No load speed for the 25 volt run is 215rpm and maximum HP occurs at approximately 115rpm giving about 6% error from ideal DC motor behavior. The data in general is noisy and would later be improved upon. The noise in this case came from the load cell measurement. It was due to a slipping flex-coupling between the motor and the dyno shaft. The power supply used to power the brake was a 0-40 volt, 0-20 amp power supply which did not have a very good fine voltage regulator to regulate the voltage going to the PAU. The following test would involve a bigger motor, a cleaner flex coupling, and a linear laboratory power supply with a better fine voltage regulator.
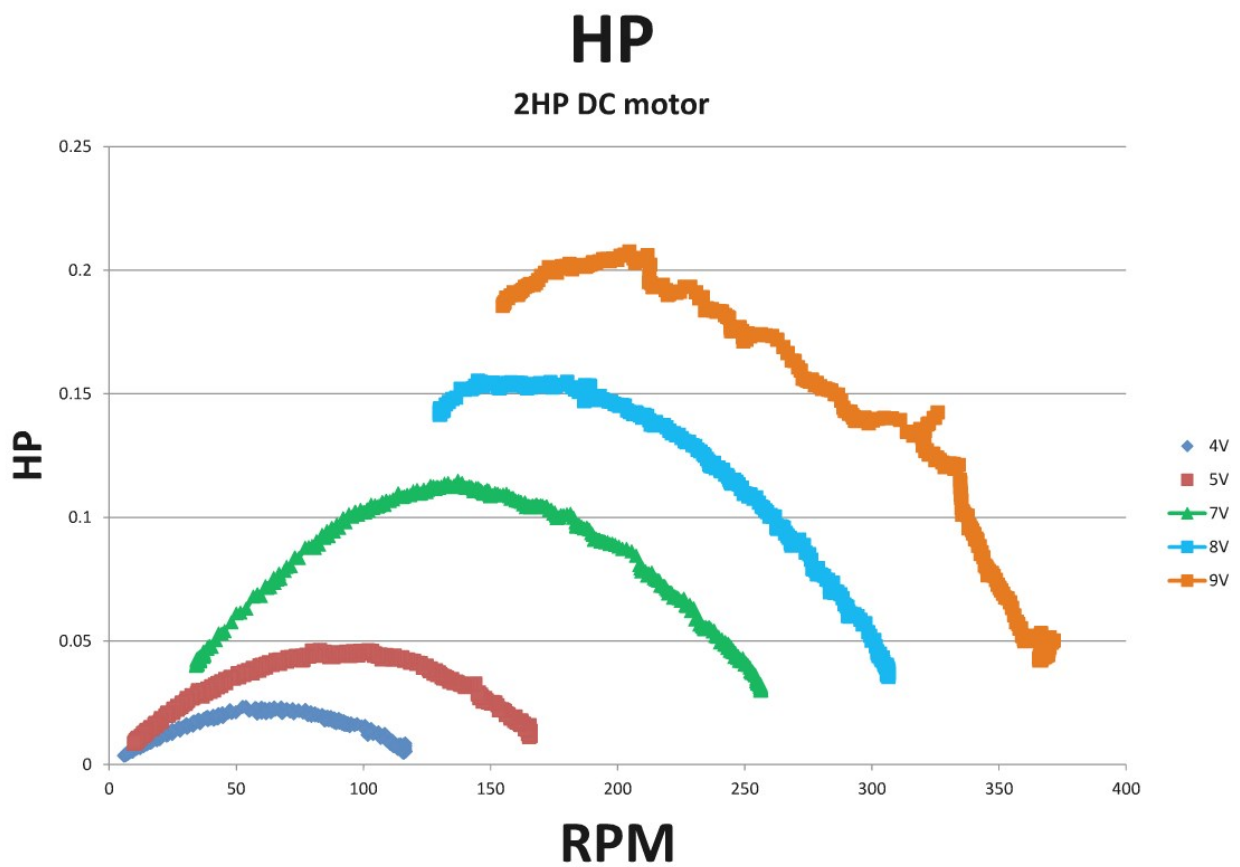
Figure 9: HP vs RPM data for 2hp DC motor
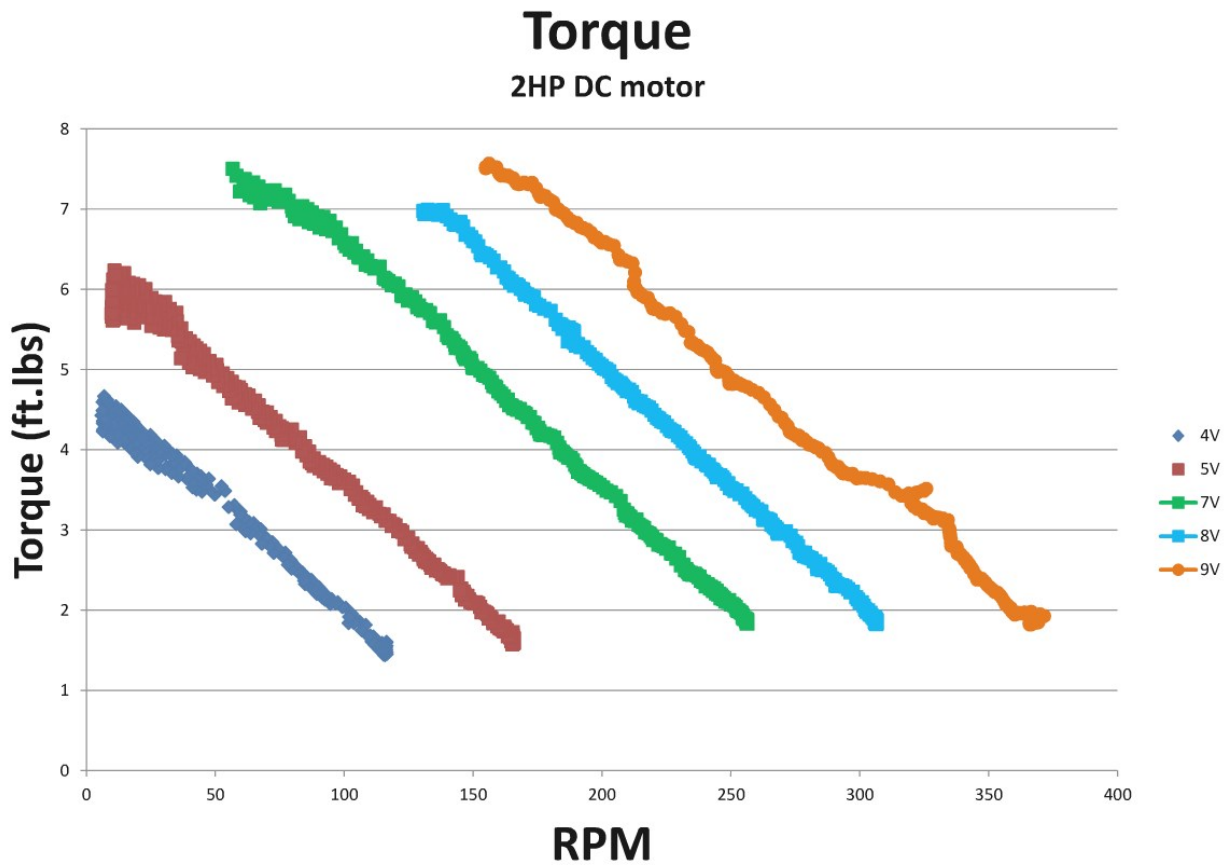
Figure 10: Torque vs RPM data for 2hp DC motor

The measurements from the 2hp motor produced much cleaner data. A consequence from using the smaller, finer power supply was that it was not strong enough to bring the 2HP motor to stall at higher motor voltages. Yet we still see nice linear torque curves and parabolic HP curves. The 7 volt motor run produced a no load speed of 278rpm. Its maximum power occurred at 141rpm, giving a 0.95% error from ideal DC motor behavior. This is quite a good calibration and gives confidence in the dynamometer's fidelity in data acquisition.

Experimental Setup Drawbacks

There remains however one small caveat that can be seen in both Figure 8 and Figure 10. The torque data for both DC motors deviates from the linear trend slightly at low rpm (yet well above stick-slip rpm). This could be the result of an imperfection in the motor performance, but the consistency of the issue across multiple tests and two different motors leads me to think the problem rests with the dyno. This issue was explored by turning the PAU off and simply spinning the rotor faster with no load to measure the load of the bearings.
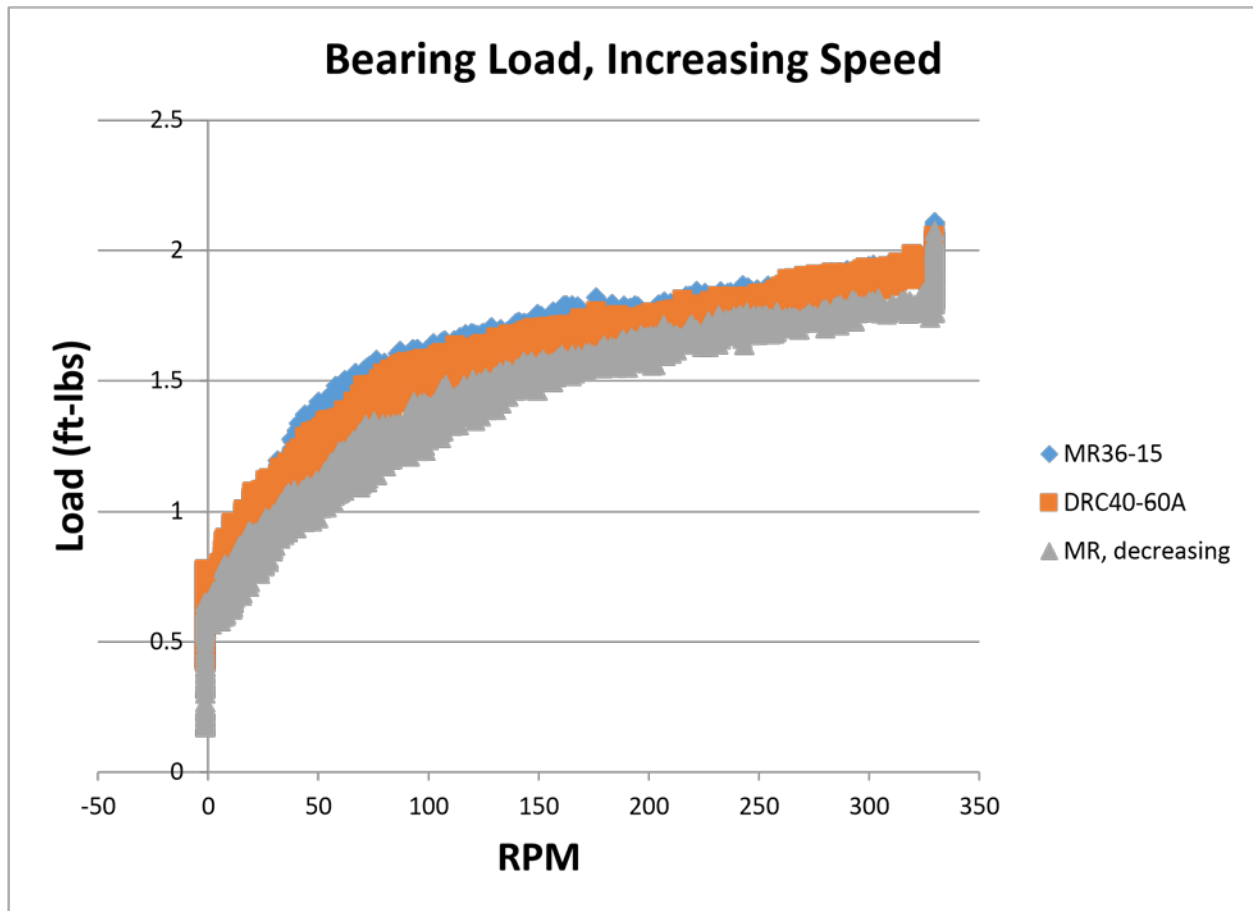
Figure 11: A measure of the load produced exclusively by the dynamometer bearings. Various curves represent data taken with different power supplies.

It can be clearly seen from Figure 11 that the slope of the load produced by the bearings in the dyno changes at around 80rpm. This is likely the cause of the deviation from the linear profile in Figure 8 and Figure 10. Thankfully most of our relevant data involving an IC engine occurs at higher speeds than 80rpm.

Another similar issue that needs to be noted has to do with the manufacturer's design of the PAU. As described in the introduction, eddy currents can form in any conductive material. However once that conductive material also becomes magnetic (which can happen when a ferrite material is exposed to magnetic fields for an extended period of time), it can possibly cause unwanted forces picked up in the measurement. Making the rotor out of steel was a poor choice because steel can become magnetized when it sits in a magnetic field like it does in the PAU. Residual magnetism in the rotor means the system deviates from eddy current behavior and toward electric motor behavior. In other words, if the rotor were highly magnetized, it could spin on its own in the presence of a changing magnetic field. Such an effect could produce similar results to that of Figure 11. A better design for the dyno would have been to make the rotor out of a conductive yet nonmagnetic material, such as aluminum or copper.

Making the rotor out of aluminum would also allow the system to respond more readily and accurately to transient stimuli such as a constant speed test when the engine is taken from no load speed all the way to stall. When the rotor is made out of a heavy material such as steel, the PAU actually consists of a combination of an inertial and eddy current PAU. Newton's second law states that an object's mass represents the proportional relationship between an applied force and the resulting acceleration (F = ma). Applying this law to a rotating object reveals that every object has a corresponding rotational inertia that relates an applied torque to a resulting angular acceleration (T = J*α). The problem with this is that the rotational energy stored in the flywheel of the dyno rotor is dissipated into the PAU through the load cell during constant speed tests. This external energy from the flywheel actually results in slightly higher torque measurements than the engine is actually producing. An aluminum flywheel would protect against both residual magnetism and against high inertial loading effects.
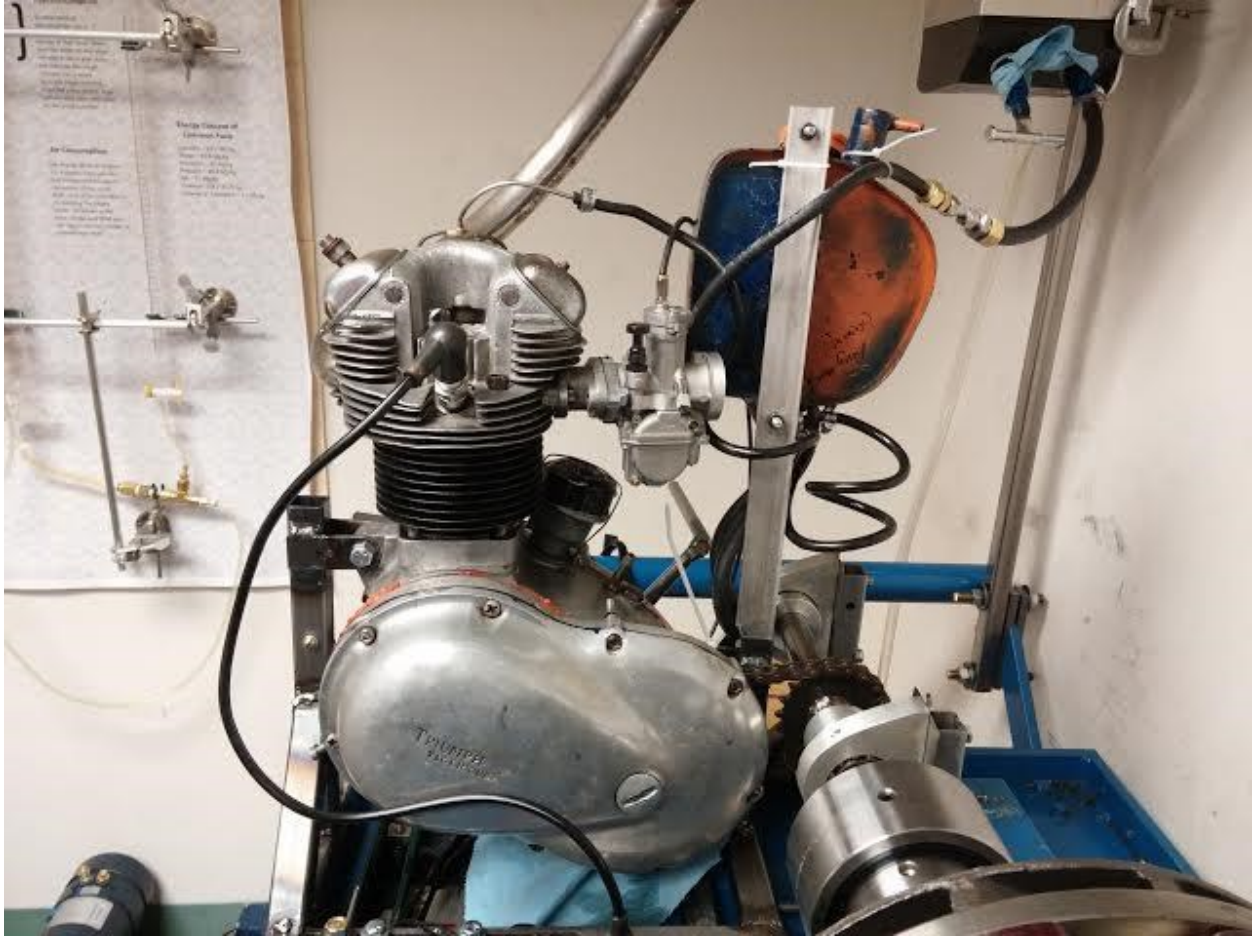
Chapter 2: Internal Combustion Engine Tests

Vibrational Signal Noise Issues

The following presented data is taken from a 1954 Triumph T20 single cylinder motorcycle engine. The engine comes from Professor Littman's freshman seminar, *The Art and Science of Motorcycle Design*. Acquiring good data on this engine has proven to be far more difficult than the electric motors. First, an engine stand had to be manufactured around the engine block to hold the Triumph engine securely on the dyno. Second, because it is an IC engine, it is very loud when operated and shakes much more than a DC motor. It is not meant to be rigidly mounted as is required for dyno operation, which means that the full intensity of its vibrations are sent into the test beds and into the data acquisition equipment. Third, this model of Triumph engine is single cylinder, which means that there is no form of mechanical stabilization of the engine, causing it to shake quite a bit. Forth, it is also much more powerful than any of the DC motors used, topping out around 10HP compared to 2HP in our biggest DC motor. This increase in power has also exposed shortcomings in our dynamometer. While the PAU is plenty capable enough to bring the engine to stall, the frame of the dyno is insufficient for the amount of vibration that the

engine produces. While most industrial dynos are built upon a bed of steel that is firmly founded in the earth, our dyno is portable: a steel bed mounted upon rubber-wheeled casters in the second floor of an academic building. Furthermore, most industrial tests involve a steel foundation for the engine that is separate from the foundation of the dyno.

Data

In the early stages of our testing, the engine was mounted directly on the frame of the dynamometer as shown in Figure 12. The engine had no trouble shaking the dyno frame which caused the load cell signal to pick up all of the unwanted vibrations. The first successfully gathered data on the Triumph engine can be seen in Figure 13. While the moving average tracks a pattern that might possibly look like a real torque curve, the data is obviously very noisy. Many load cell measurements actually maxed out the 5 volt max on the cell making it so that data cannot even be represented.
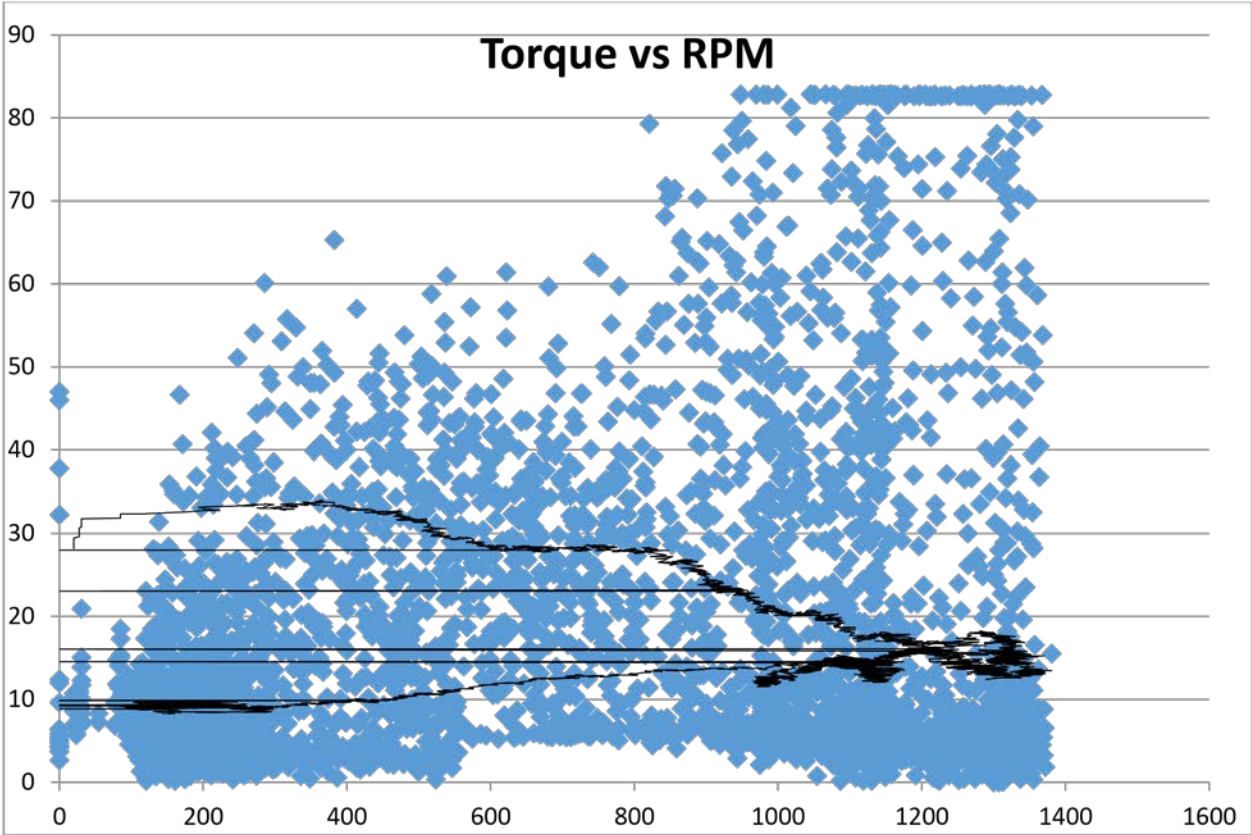
Figure 13: Triumph engine torque data, first successful data acquisition

While Figure 13 does not represent the desired result, it did represent a milestone in the development in the engine dynamometer laboratory. Data had never been acquired using an IC engine before with that dyno, because the equipment had not previously been manufactured to

accommodate such an engine.[1] The victory was short lived however, as gathering good data and simply gathering data are two entirely different things.

Data Acquisition Improvements

The first attempt at improving the acquired data was to change the axis of the load cell mount. The rational for this was the fact that the load cell mounting used in the data in Figure 13 was a vertical mounting which is directly in-line with the engine's single cylinder axis, as can be seen from Figure 12. The theory was that the primary source of the vibrations was coming from the firing of the engine's single piston. Because these vibrations were concentrated within the same axis of the load cell, the load cell was picking up the full magnitude of the vibrations. A new mount for the load cell was then manufactured so that the load cell could sit horizontally, 90 degrees out of phase with the piston's axis. The data from the horizontal load cell test can be seen in Figure 14. The dip around 1500 rpm was due to spark misfiring which was observed during the test. The X axis is dyno rpm, Y axis is load cell voltage. The only thing that appears to be better about this data is the moving average. While the spread of data is quite large, with many points still maxing out the 5 volt load cell, the moving average tracks a torque curve that looks more believable.
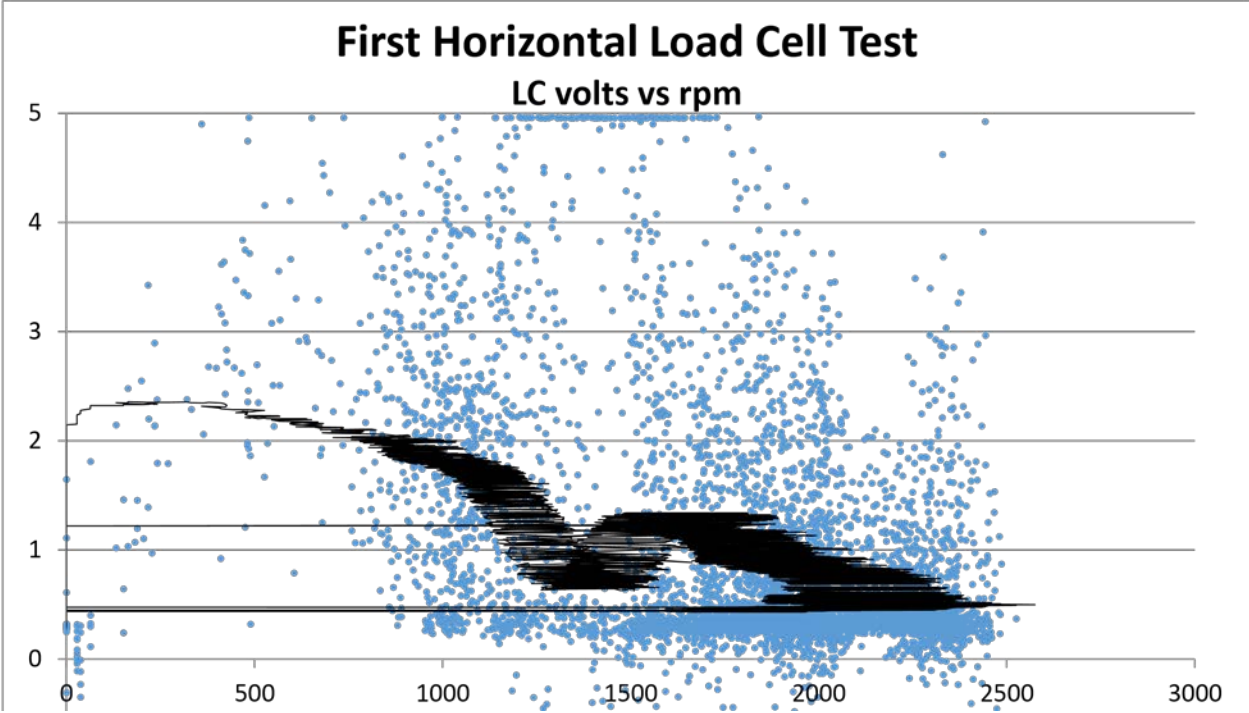
Figure 14: First horizontal load cell data acquisition, load cell data

Because the horizontal load cell configuration proved to not solve the signal noise issue, it was decided that the engine needed to be separated from the dynamometer completely. The engine needed its own, heavy stand that could withstand the vibrations caused by the engine and isolate

---

[1] To see details of my manufacturing of laboratory equipment, please see Appendix E.

them from the data acquisition equipment on the dynamometer. As such, the engine was moved to an old milling machine base which proved to be a perfect platform because it offers both a heavy base and a 3-axis fully adjustable stage to aid in positioning the engine with the dyno drive sprocket. The drive chain was lengthened to reach across the two stands to drive the dyno drive sprocket as seen in Figure 15.

Although the engine and dyno were now separate, the portable feature of the dyno continued to be a problem. The engine on the milling machine base wanted to pull the dyno stand closer with it when the engine was under load, which loosens the chain and ruins the test. Because of this the two stands needed to be stood off from one another, again introducing a connection between the engine and the dyno stand, however a less intimate connection than before. The engine was stood off from the dyno with two shock mounts which both kept the two stands from being pulled together and dampens the vibrations between the two stands (see Figures 15 and Figure 16). Because of such an orientation, the vibrations then began being translated to the dyno primarily in the horizontal direction (although many vertical vibrations from the cylinder were still being translated through the laboratory floor). With the new mounting configuration, it became necessary to determine whether the horizontal or vertical orientation of the load cell was going to be best suited for gathering data and minimizing measured vibrations. After several tests it was apparent that under the new configuration, large vibrations were transmitted
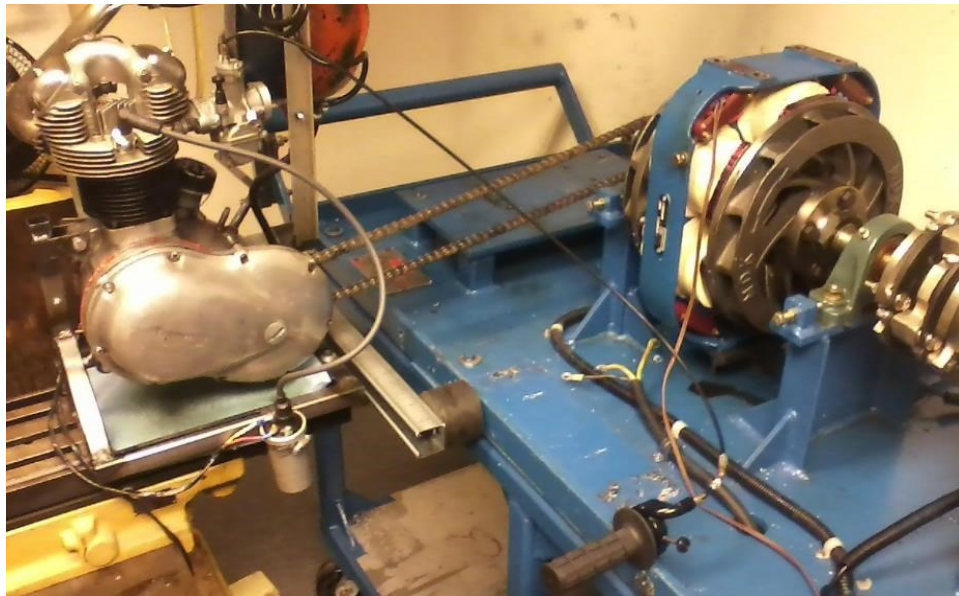
Figure 15: Engine and dyno separated on two separate stands

Figure 16: Close up of engine standoff and shock mounts

horizontally through the test equipment, and smaller, more consistent vibrations were transmitted vertically through the floor. Therefore the vertical load cell mounting was chosen to proceed with data acquisition.

Factors successful at noise reduction:

- Isolating engine and dyno (with all DAQ instruments) on two separate stands,
- Using engine shock mount stand-offs between the two stands,
- Isolating the primary vibrational axis and the load cell axis orthogonally to each other.
- Shutting off the AC power supply after the AC motor was finished starting the IC engine.
- Turning off cell phones while data is being acquired. In the days of bad cell phone service in the Equad, the "searching for service" signal that the wireless carriers send out was being picked up by the antenna that our load cell wire created, resulting in a pinging of the load cell data. This wire carries the most sensitive part of the data, and was therefore strung up through the roof over to the DAQ card to keep it away from any AC signals.

Factors that were unsuccessful at noise reduction:

- Preloading the load cell. Because there is no damper on the load cell shaft, more mass just meant higher amplitude peaks on the signal noise. Preloading made the signal noise worse.
- Jacking the stand up to rest on 4x4 wooden blocks rather than on wooden casters. Although this seemed to be a good idea to give the dyno a more solid foundation on a surface rather than on a line support, this change had no effect on the level of load cell signal noise.

Chapter 3: Data Filtering

Justification

While many laboratory adjustments were effective at reducing some of the signal noise generated by the single cylinder Triumph engine, the surrounding environment of the lab itself is ill-equipped to properly handle the data acquisition. While the dyno test bed and the milling machine base are both quite massive and separate stands, they are not massive enough. Even if massive enough bases could be utilized, the vibrations still go through the second-story floor which couples the two stands even in the absence of physical couplings. Vibrations therefore are still transferred vertically into the axis of the load cell, which also effects the fidelity of the variable reluctance rpm signal. Until a new location for the dynamometer can be found, ideally one outside where two separate massive foundations can be laid into the earth, data filters will need to be used in order to extract curves for comparison to Triumph Bible results and engine modeling software.

Methods

The following filtering methods were applied to data acquired from the 60 tooth variable reluctance rpm pickup and the 50mV/lb load cell mounted vertically; acquired by way of separate engine and dyno stands coupled horizontally through engine shock mounts.

When filtering data, a decision must be made as to whether filtering will take place mid-acquisition, post-acquisition, or during both phases. When looking at a messy plot such as the one in Figure 17, the quick fix toward getting better data would be to simply program the DAQ system to sample the data at a slower rate in order to record less points. While this is easy and pretty, the resulting data will likely not truthfully represent the studied system. Sampling data at a slower rate only means acquiring less points, which means it could be acquiring all the wrong (noisy) points.

The next best mid-acquisition filtering technique is to sample the data at a slower rate and to average the data in-between clock ticks in order to generate one reported data point. While this method is better than the previous, it still poses some serious limitations. Firstly, mid-loop averaging can slow the system response time and result in missing data or lagging data. Secondly, while mid-acquisition averaging is generally effective for quasi-equilibrium systems, measuring an engine's torque curve results in transients that are too drastic for a pre-set averaging domain to be set. Engine rpm and load are changing at non-steady rates and therefore a pre-set averaging domain would result in either under or over averaging in certain data regions. Considering these things, it seemed like the best form of data filtering for this system was post-acquisition only. Therefore the sampling rate of the DAQ was set to sample data at a very high frequency in order to be sure to capture the details of every transient in the system. An example of the raw data to be filtered is shown below in Figure 17. This data was sampled at a rate of 100 times per second.
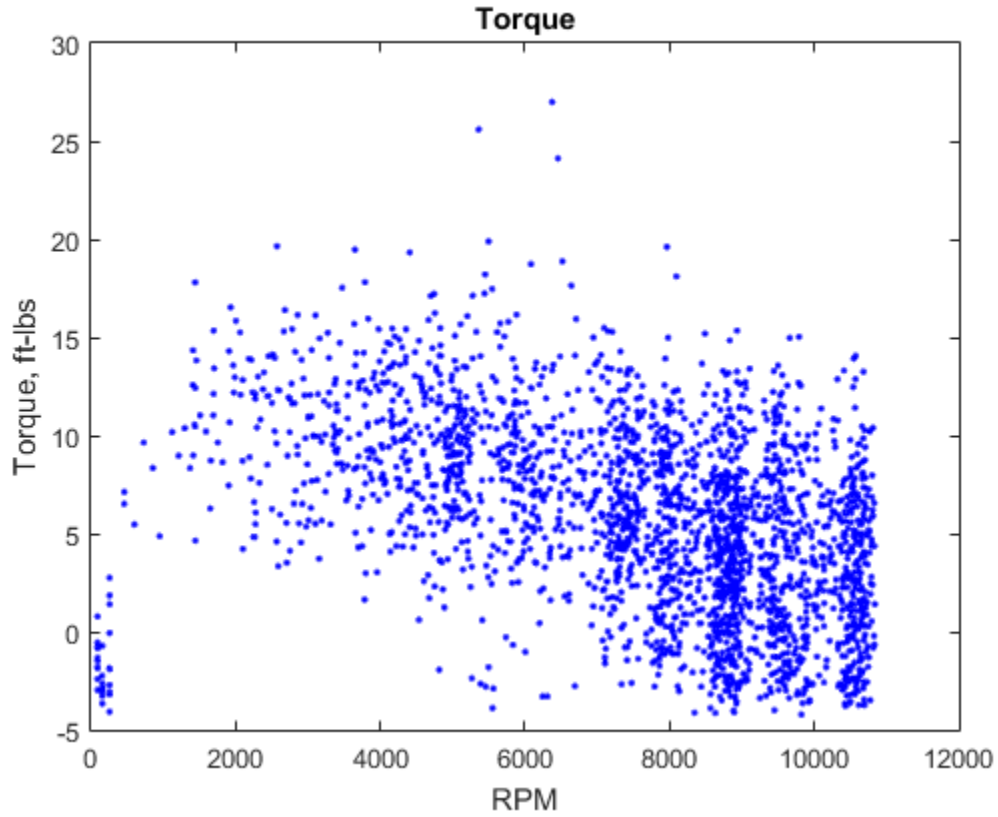
Figure 17: Raw torque data (from Triumph engine)

The first step in designing an effective, reliable data filter is to look at the derivatives in the data in order to determine where the majority of the variability is coming from. A plot of the RPM and torque derivatives is shown in Figure 18.
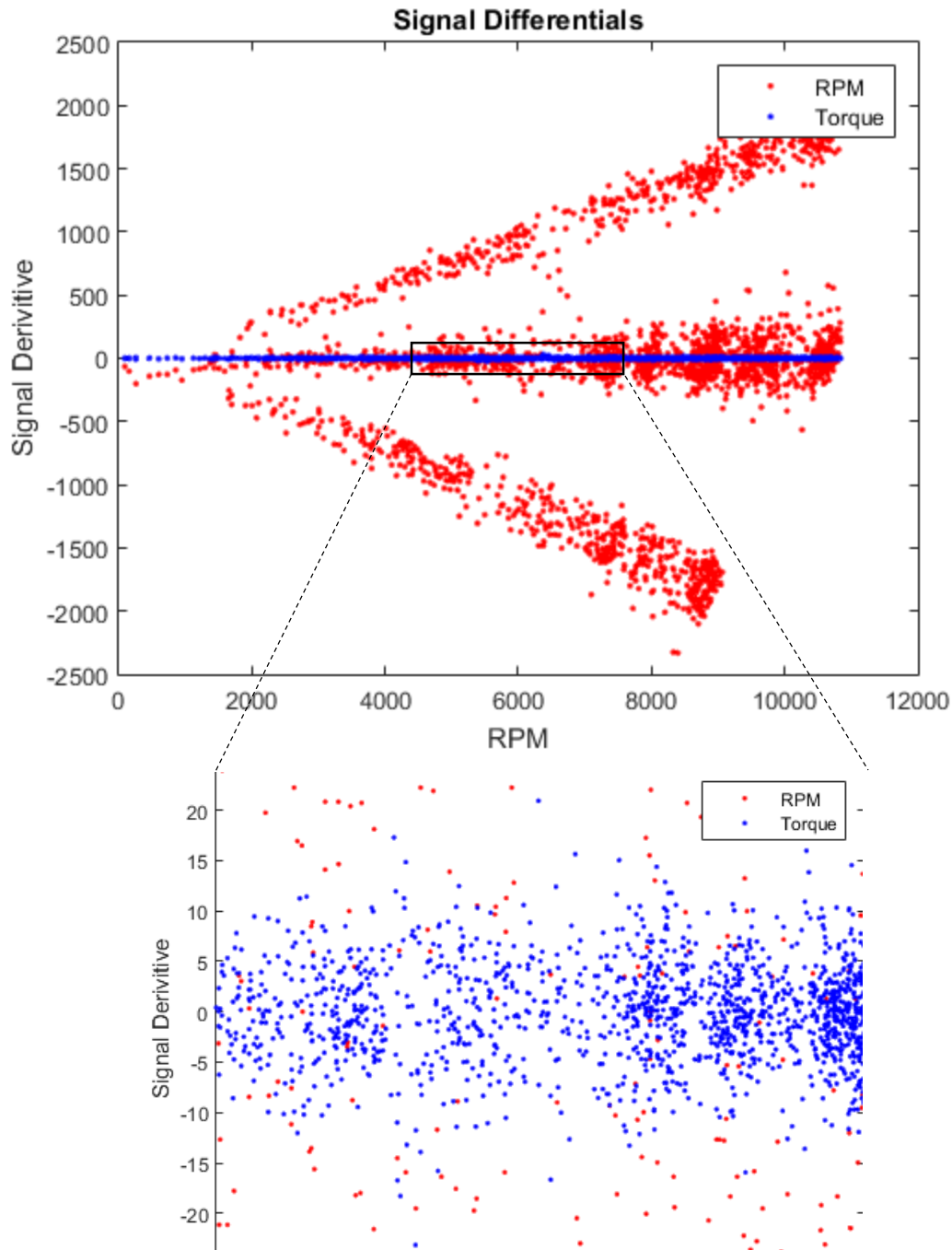
Figure 18: Raw data signal differentials

The derivative plot shows that the load cell signal noise is quite predictably between -10 and +10 ft-lbs, while the rpm noise follows a more unusual trend that varies with rpm.

The benefit of developing a post-acquisition filter as opposed to a mid-acquisition filter, is that during post-acquisition it is possible to design a filter to accurately represent the transients in the system as to avoid misrepresenting the data by using a mid-acquisition filter with a static domain. In other words, sampling data slower and averaging the points in between will always consider

the same number of points per reported data point, regardless of the range of rpm or load cell data acquired during the interval. The benefit of a post-acquisition filter is that the length of the intervals used for signal averaging can be determined in order to match the transients in the specific data. The way this is done is by, after acquiring data, partitioning the rpm axis into a desired number of segments, *dx.* The choice of a good *dx* length has to do with consideration of not choosing a length so large as to over average the transients in the data, but also not so small as to not achieve any filter at all. A choice of dx = 250 rpm was made in the current filter in order to match the rpm step length used in the Virtual4Stroke engine modeling software. Thus an rpm range of 10750rpm was partitioned into 43 segments.

The next step is the crucial step to accurately representing data transients. For each *dx*, the number of data points sitting within each dx are counted and the number stored. The output from such a process for the raw engine data is shown in Figure 19.

# of data points	RPM range	# of data points	RPM range	# of data points	RPM range
116	10750	50	7000	20	3250
166	10500	27	6750	22	3000
54	10250	39	6500	19	2750
60	10000	43	6250	18	2500
91	9750	54	6000	16	2250
141	9500	56	5750	13	2000
63	9250	35	5500	8	1750
171	9000	50	5250	11	1500
229	8750	77	5000	3	1250
85	8500	52	4750	2	1000
72	8250	38	4500	2	750
132	8000	46	4250	3	500
70	7750	32	4000	3	250
99	7500	33	3750		
115	7250	23	3500		

Figure 19: Number of data points per filter interval

What can be seen here is the amount of data that was taken for every rpm interval. Because the data is manually acquired and not automatically controlled, the engine is not going to go through each rpm range at the same rate, but rather it will look something like the layout in Figure 19. It's also easy to see here what the danger of mid-acquisition filtering is. For instance if a sampling rate of 100Hz for an arithmetic averaging filter is set in your DAQ system, it will accurately represent the data at rpms of 10750, 9750, 7250, (rpm intervals that have ~100 data points in them) and that's about it. But the next time data is acquired it will be spread out differently again. An example of over averaging comes into play when there are fewer data points per interval. For instance a sampling rate of 100Hz in the data above would average all acquired data from 250 to 3000 rpm and lump it into 1 data point. Here the transients are faster than the sampling rate. An example of under averaging would arise at around 10500, 9500, 9000, and 8750 rpm where the transients in the system are slower than the sampling rate. This is a better situation than over-averaging, but it is still inefficient. By using post-acquisition filtering techniques, the sample size for each rpm range can be perfectly determined in order to filter the data efficiently while not misrepresenting any transients.[2]
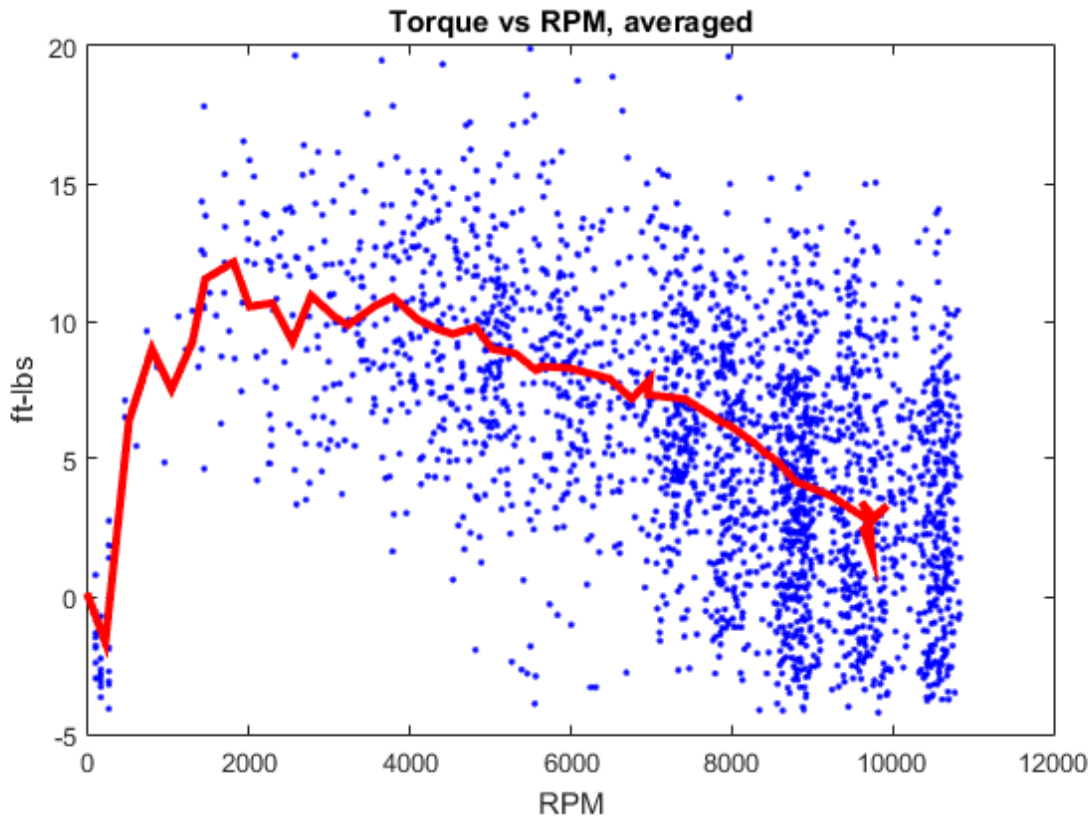
Figure 20: Filtered data with preset sample size for every rpm range

---

[2] One way to use this technique for a mid-acquisition data filter would be to use the square wave generated by the rpm variable reluctance pickup as an external clock for the LabView DAQ card to generate sample size. Then, a sample size can be pre-set and will accumulate at the same rate as the rpm transient, thus assuring that there is no under or over-averaging of data. Although noisy rpm data is the result of a non-uniform square wave, therefore using such a wave as an external clock could be problematic for generating an accurate sample size as well.

By averaging the load cell and rpm data for the sample size at each rpm range listed above, the following curve is extracted and shown in Figure 20. The curve is further smoothed using a 3-point moving average. The final smoothed curve is shown in Figure 21.
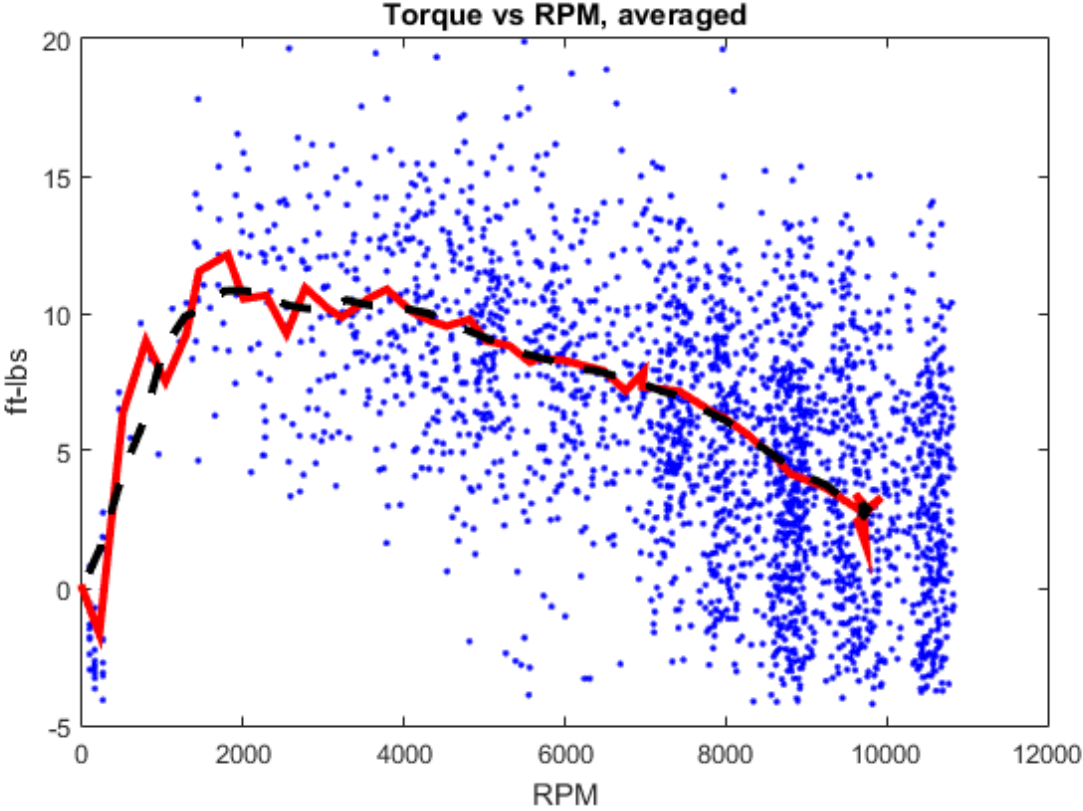
Figure 21: Filtered data. Red line represents the weighted average. Black line represents the result of a 3 point moving average to smooth out the jagged edges of the weighted average

The benefit of a variable, controllable sample size for each rpm range (dynamic filter) can be seen graphically when compared to a moving average that is applied with a fixed filter domain (static filter). What results is a curve that misrepresents the raw data because of a disproportional locational distribution of the data. Because this particular data is denser at high rpm and sparser at low rpm, data is over averaged at low rpm and under averaged at high rpm, as can be seen from the green line in Figure 22. The final filtered data using the dynamic filter plotted on top of the raw data can be seen in Figure 23.
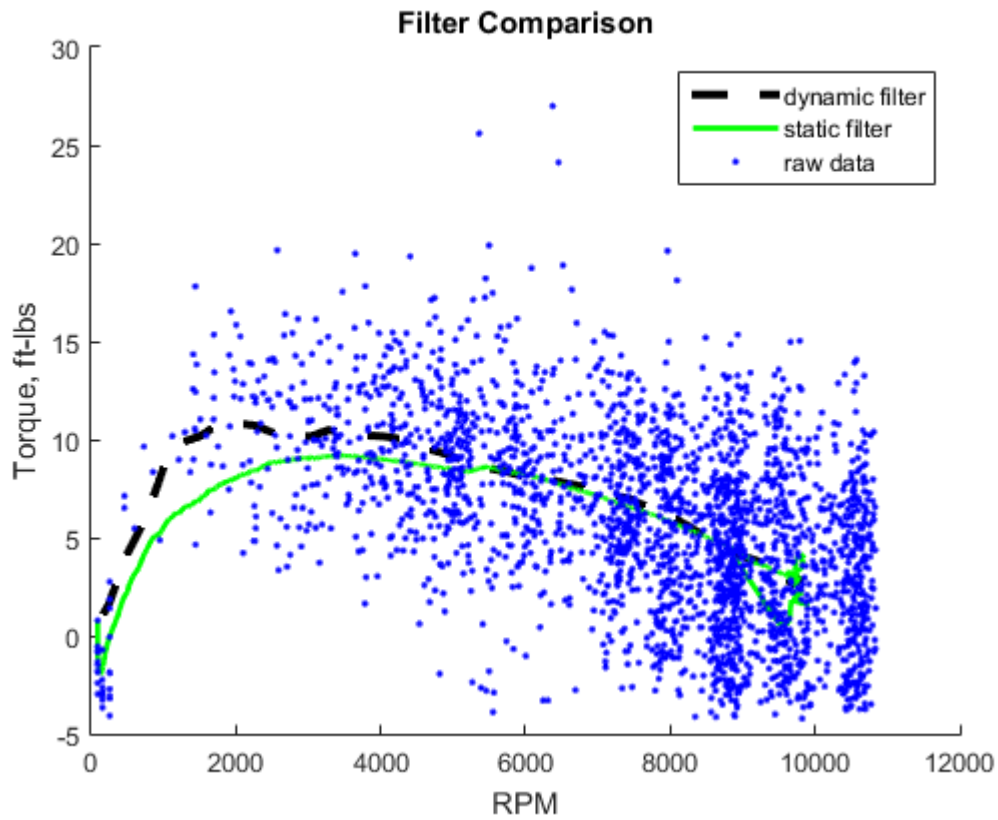
Figure 22: Static vs dynamic filter comparison. The filter generated in this paper is the dynamic filter represented by the black line. In the static filter (green line) over-averaging is observed at high rpm where the curve traces back and around itself, and under-averaging is observed at low rpm where visually the line miscalculated the trend of the data.

Filter Results
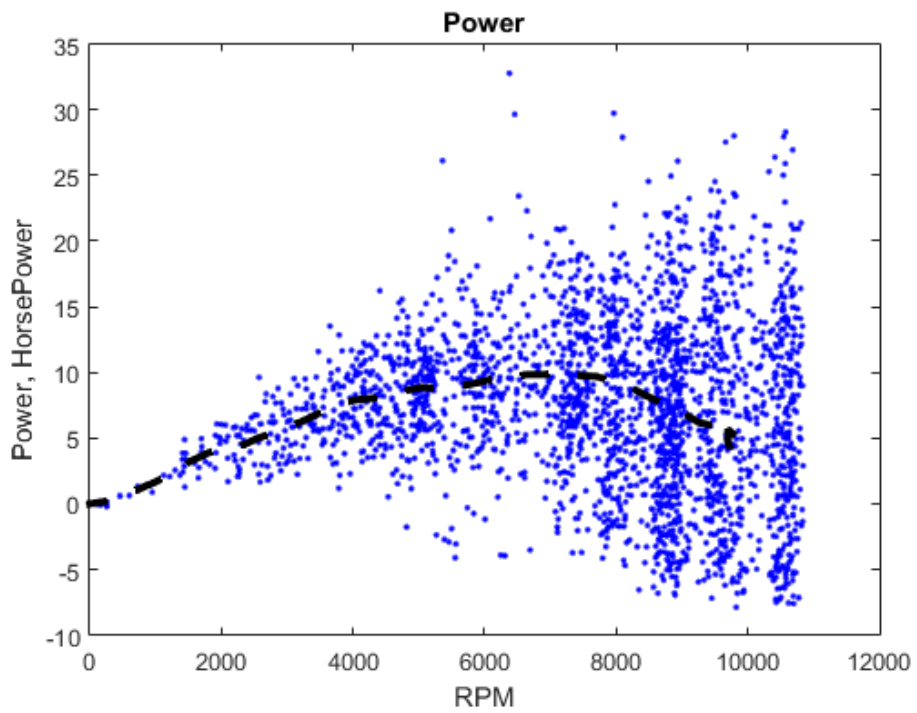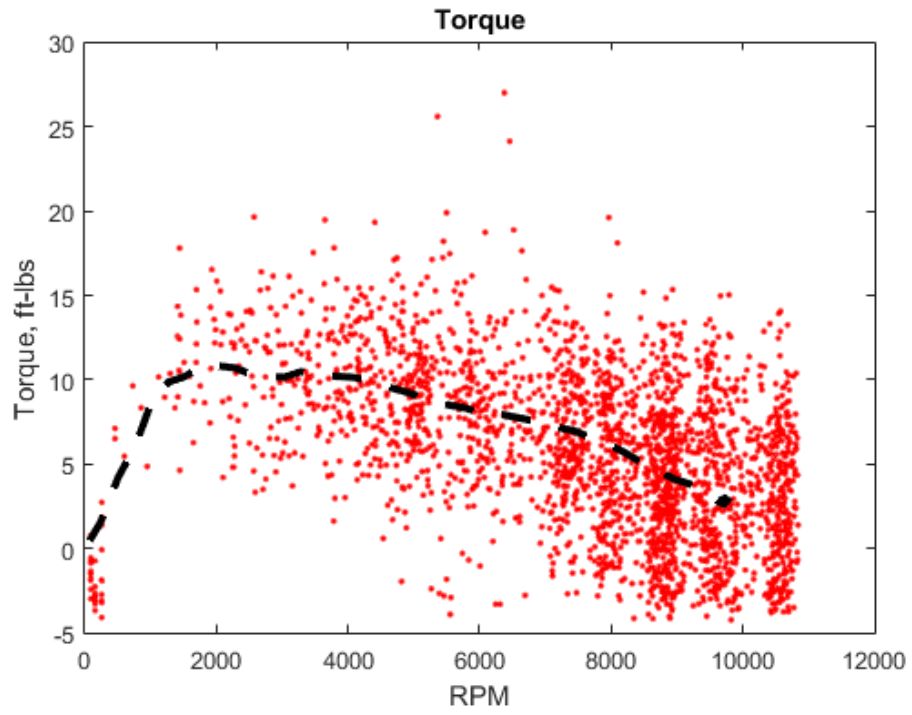
Figure 23: Raw data, filtered using dynamic filter

Chapter 4: Comparison to Engine modeling software

Virtual4Stroke Software

Virtual 4-Stroke® is a powerful engine performance simulation software developed by the Optimum Power Technology company. It designs, simulates, and optimizes engine geometry in an accurate, fast, and user-friendly virtual environment.[viii] The software is currently installed on the 64 bit, 2.6 GHz processing computer in the Mechanical and Aerospace Engineering Lounge and is used as the main source of data verification in this paper. The software allows you to design and specify all the geometric and thermodynamic parameters of your engine and fuel, and then integrates thermodynamics, fluid dynamics, and CFD to calculate engine performance. An instruction manual on how to operate the software is included in Appendix A.

Triumph Engine Model

Nigel Brauser, a Mechanical Engineering student at Princeton, class of 2013, made a considerable effort to disassemble the Triumph engine and accurately measure its different mechanical components for editing the engine geometry inputs in the software. The work done in his senior thesis is the basis for the work done in this section. He was able to put together an engine model using the measured engine components which generates software output that we can assume is the most accurate representation of the expected torque and power curves for the Triumph engine. A list of variables, values, and the flow diagram for the triumph engine model are included in Appendix B.

Two small modifications to Brauser's engine model were made to better fit this year's model. One of the modifications was a corrected error, the other a representation of a change in the engine. The error in Brauser's model was the spark advance profile. Work done in Professor
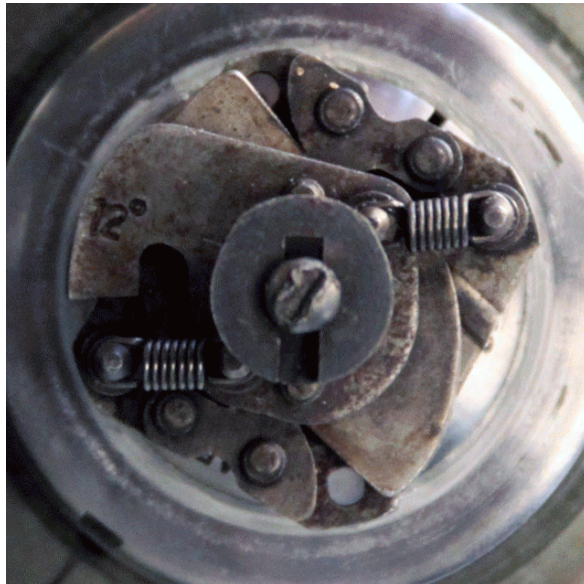
Figure 24: Top view of '56 Terrier distributor showing the spark advance mechanism

Littman's Freshmen Seminar course, *The Art and Science of Motorcycle Design,* on the distributor on the 1956 Terrier Motorcycle model helped to pinpoint a more exact curve for spark advance. The mechanical spark advance mechanism in the distributor is operated purely by centrifugal force that results from the spinning crank shaft while the engine is running. A network of weights and springs in the distributor expand outward due to centrifugal force as the engine speeds up and the distributor rotates faster, advancing the contact points forward until a mechanical stop limits the advance to 12 degrees. The class also did some research to deduce that the spark advance varies linearly with rpm, until about 2000rpm when the mechanical stop is engaged and spark advance remains constant throughout all higher rpms.[ix] This information was corrected on Brauser's engine model, which had a linear spark advance profile gaining to 28 degrees advance at 6000 rpm. It is important to note that in the updated engine model, the zero rpm advance is set at 4 degrees, which is recommended by the Triumph shop manual.[x] Therefore the engine gains 12 degrees advance, maxing out at 16 degrees advance at 2000 rpm.

Apples to Apples

Because the engine dynamometer measures torque and rpm at the tail end of the power train whereas the Virtual4Stroke engine modeling software only derives the torque produced directly in the engine's cylinders, it is important to scale the data measured on the dyno to reflect the data that would be directly measured from the crankshaft before engine data can be compared to engine modeling software. Inside the engine's cylinder, torque is generated through the forceful displacement of the piston via combustion combined with the leverage gained through the off-center linkage of the connecting arm with the crankshaft, thus translating linear piston motion into rotational motion of the crankshaft. The torque here goes through a primary reduction as it enters the clutch basket, which is a 1.5/1 ratio in our Triumph engine model 27171. This magnifies torque while reducing rotational speed. From the clutch basket the torque passes through the engine transmission, whose gear ratio is dependent upon the gear that the engine is in.[3] The 16 tooth output gear of the transmission drives the 18 tooth dyno sprocket via a chain (or in the case of a bike, it would drive the rear wheel sprocket), which completes the power train. While in 4th gear, every 1 rotation of the engine dyno corresponds to 2.8 rotations of the engine.

Therefore in order to correctly compare any data taken from the dyno to the data generated by the software, two things have to happen after all measured parameters have been converted to

---

[3] Our engine dyno tests were done in 4th gear for a variety of reasons. First, it is easier for the AC motor on the dyno to start the triumph engine when it is in 4th gear (requires less torque during initial turnover). This more even torque ratio also allows us to achieve less rpm gain with more throttle, providing a more controllable engine during testing. 4th gear also represents the engine's direct drive, meaning a 1 to 1 gear ratio from the crank to the output gear. Operating in a 1 to 1 ratio maximizes the efficiency of the power train.

consistent units: *The dyno rpm must be multiplied by the overall gear ratio (2.8 in 4th gear) to get engine rpm, and the dyno torque must be divided by the overall gear ratio to get engine torque.*[4]

The torque and power curves generated by the Virtual4Stroke software, plotted along with the empirical data gathered from the Triumph engine on the dyno in our lab, are shown in Figure 25. The plots of their derivatives are shown in Figure 26.

---

[4] Calibration of the load cell is another important step. At the time when this engine data was taken, the load cell was producing 0.056 volts per pound. Load cell voltage needs to be converted to pounds, which then needs to be converted to ft-lbs (using the length of the dyno lever arm), which then needs to be converted to engine torque (by dividing by the overall gear ratio).
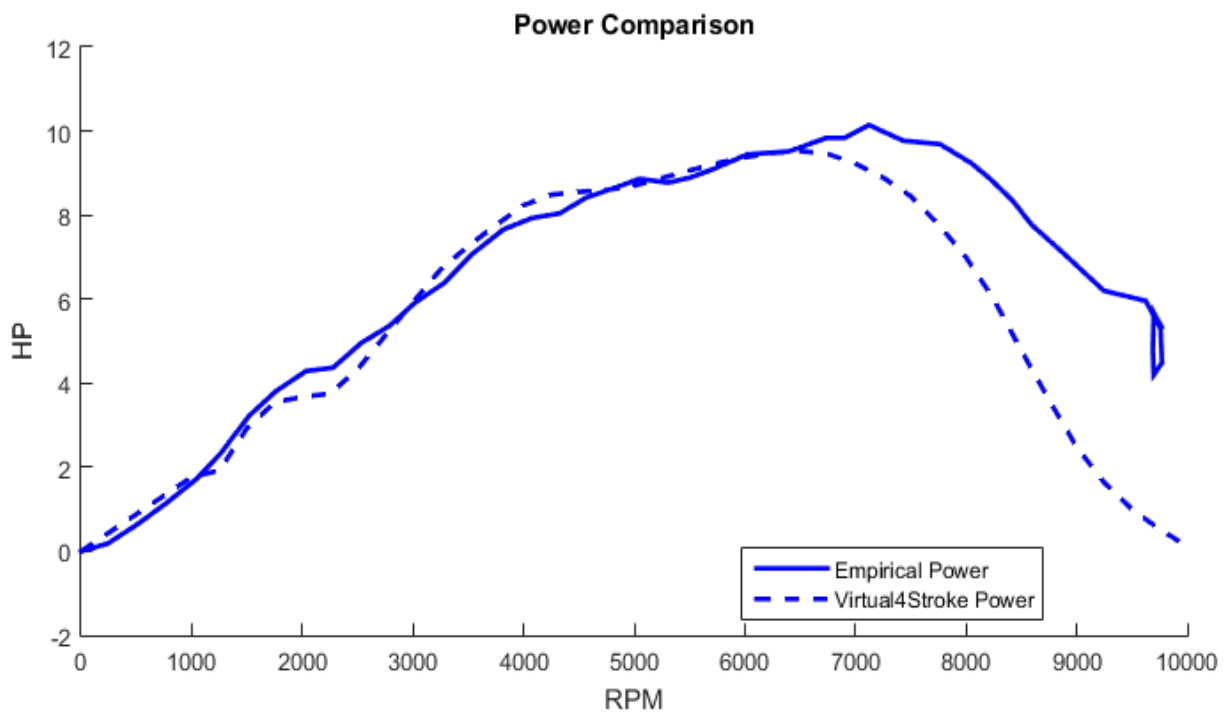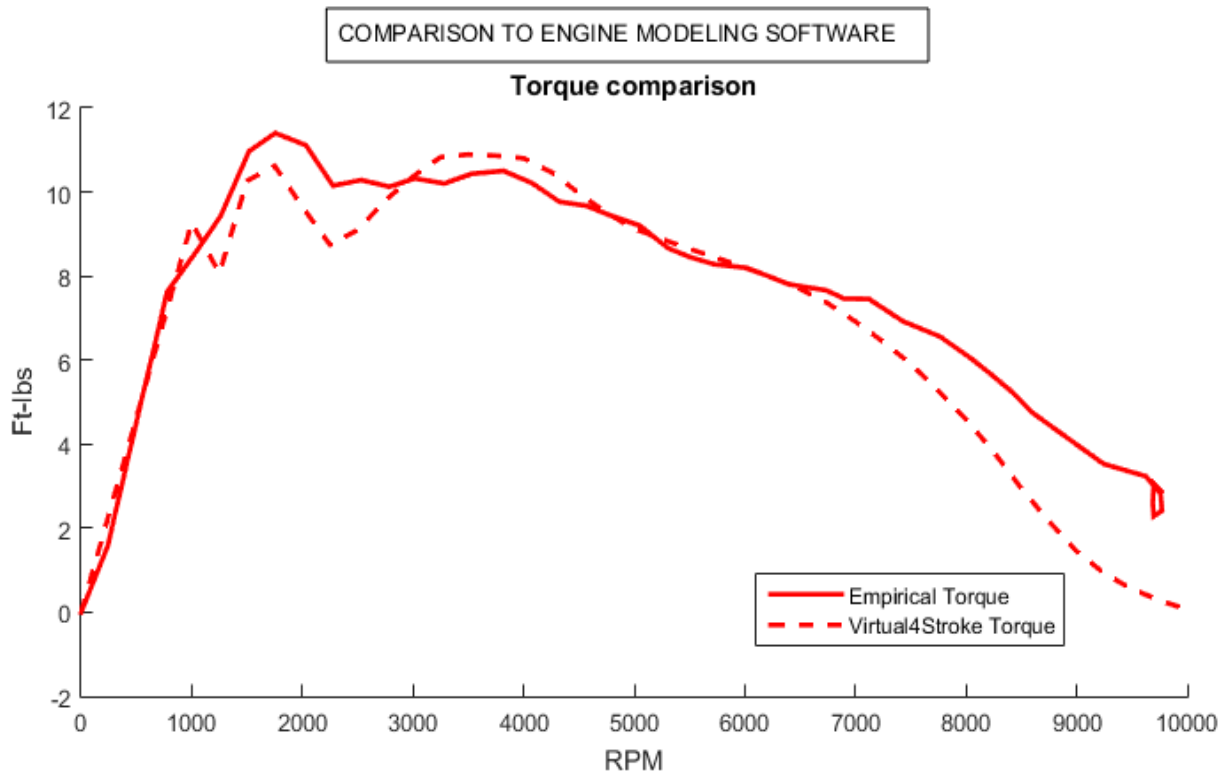
Results

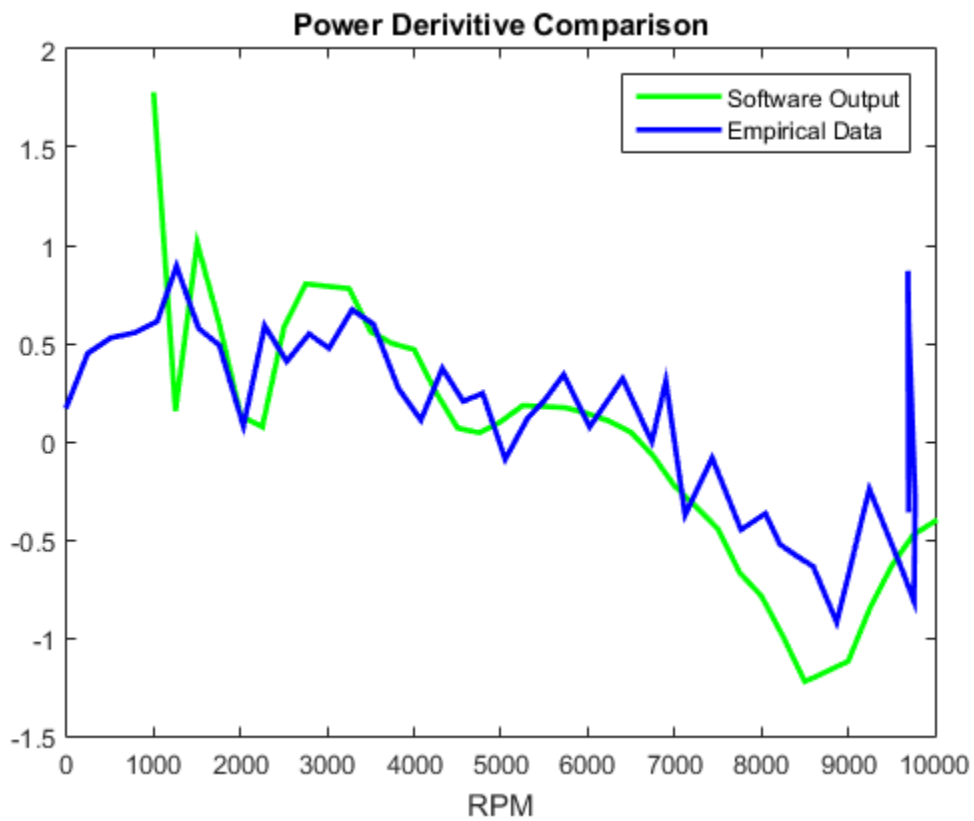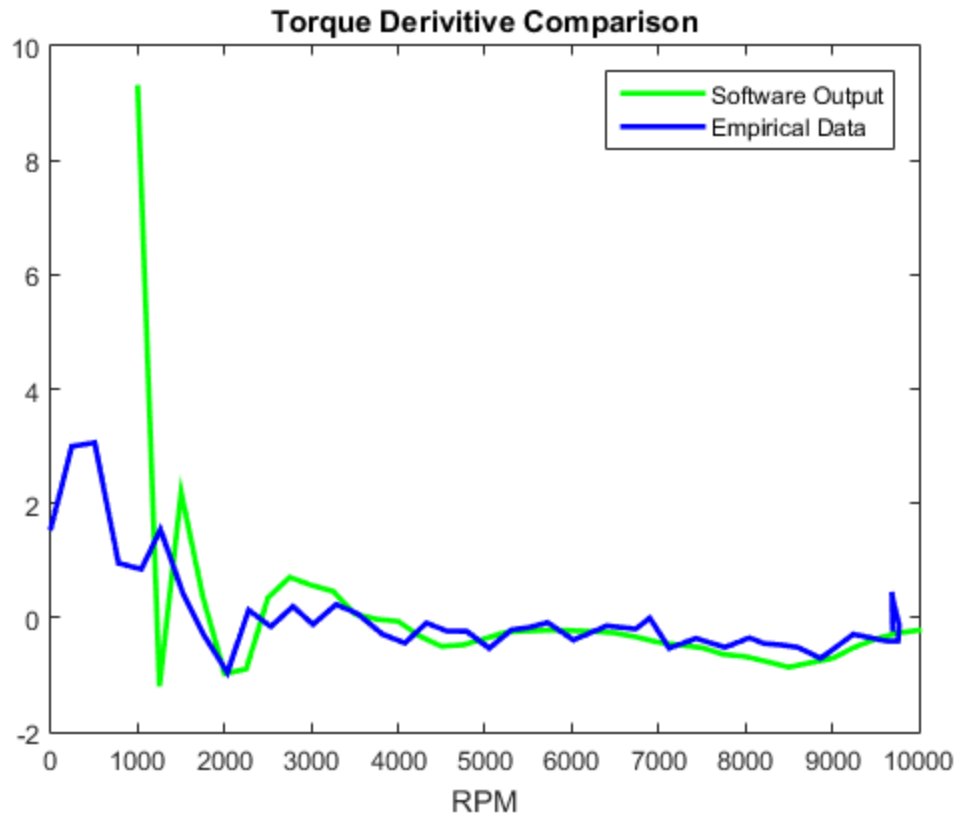Figure 25: Comparison of empirical and numerical results

Figure 26: Derivative comparison plots of empirical data and software output

Analysis

Figures 25 and 26 offer a very encouraging result. While the empirical and numerical curves in no way completely match up, it is mostly unrealistic to expect them to. Testing conditions of the engine dynamometer lab are still manually operated, less than ideal, and therefore subject to human error or at least slight variations between tests. On the contrary, the engine modeling software represents an idealized, repeatable, computational system that offers the same results every time given a consistent engine and identical test procedures. What is encouraging about the results in Figures 25 and 26 however, is that magnitudes, trends, and events all matchup between empirical and numerical results despite the curves not being exact replicas of each other.

The first encouraging discovery is that the general trend of the torque and power curves, as seen in Figure 25 and evidenced in Figure 26, almost completely match up until about 7000 rpm. This represents consistent data throughout the realistic operable range of the engine. Once above 7000 rpm, the engine gets to speeds that may be realistic for dyno tests, but not for road tests. An engine is able to be spun up to around 10000 rpm in the laboratory because very little load is applied when determining the engine's no-load speed. This load is much smaller than loads that a road bike would experience at 7000 rpm. A side effect of the fact that the range between 7000 and 10000 rpm is only possible at low load is that the engine-dyno system actually seesaws back and forth between an engine-dominated and a dyno-dominated system at this rpm range. What this means is, at times, due to the occasional miss-fire of the spark plug or an occasional lapse in power output of the engine, the engine is actually being motored by the kinetic energy stored in the rapidly spinning dyno flywheel (another reason why a steel flywheel was a bad design choice, heavy flywheel = more inertia/stored energy). This accounts for the higher torque and power output of the empirical curve over the numerical curve in this rpm range. At the highest measurable rpm ranges (around 9500rpm) even noisier empirical data is observed due to load cell signals picking up torque data that is generated from the rotational inertia of the flywheel at times and not just the engine.

The second encouraging discovery is that not just the trend of the rise and fall of the torque and power curves are consistent throughout the realistic operable range of the engine, but the resonance peaks are consistent as well. We see resonance peaks in both the torque and power curves at about 1000, 1900, 3900, and 6700 rpm which are captured in the empirical data and verified by the numerical simulation. The first resonance peak at 1000 rpm we see very unassumingly in a slight discontinuity in the empirical data just before 1000 rpm. The second resonance peak at 2000 rpm is represented very distinctly in both the empirical data and the numerical simulations, and magnitude and location are almost identical. Likewise at 3900 rpm, a resonance peak is clearly distinguished in both the empirical and numerical curves, with magnitude and location being almost identical. Finally at 6700rpm, where peak engine power is produced, we observe a 4th resonance peak in the torque curve as the declining curve slopes back up momentarily with a burst in torque.

Comparison to 1956 Data

Maximum power as calculated by Virtual4Stroke is about 10hp at approximately 6500 rpm. Maximum power as gathered from our engine lab is just over 10hp at approximately 7000 rpm. The published power curve for the Triumph T20 200cc single cylinder engine is plotted and compared to these power curves in Figure 27.
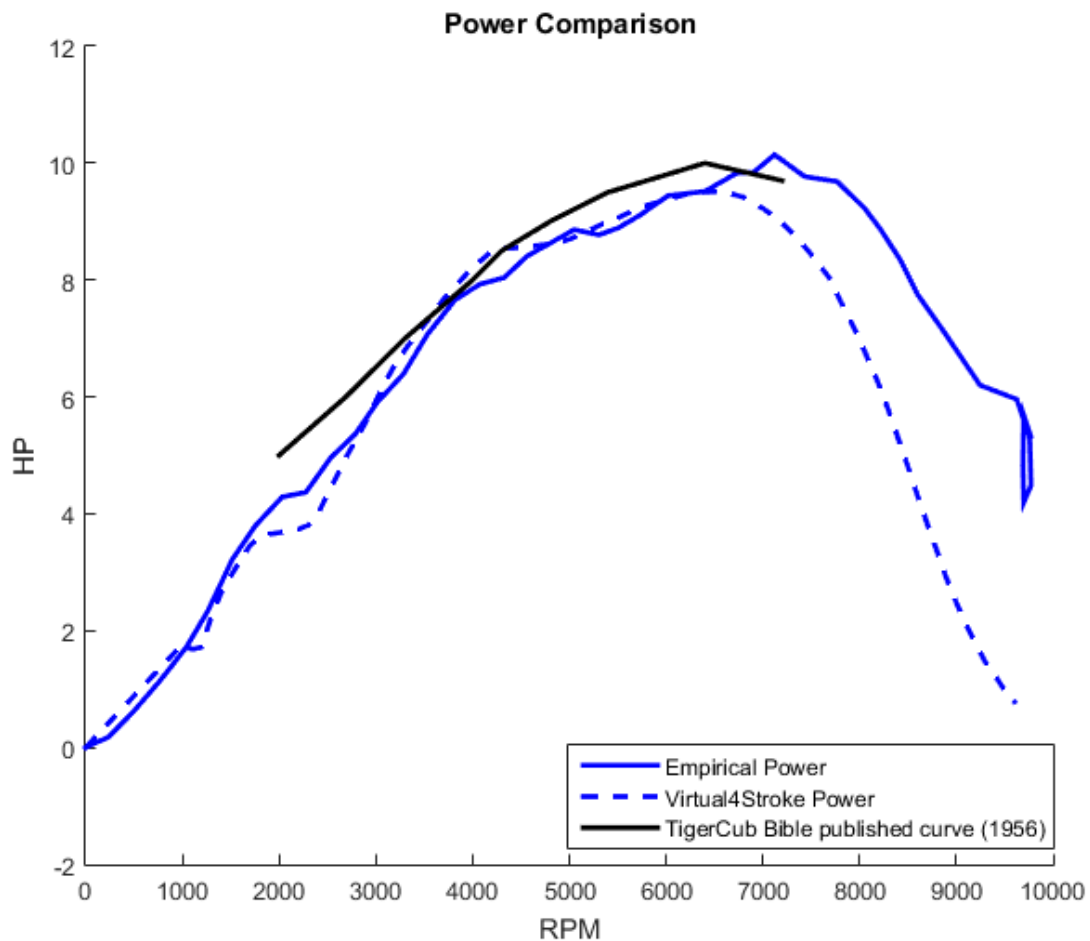
Figure 27: Triumph TigerCub 1956 published curve

The TigerCub Bible states that the T20 model makes a full 10bhp at just over 6000 rpm.[xi] However this published curve in 1956 is plotted by hand on graph paper, and no indication of the measuring method is given. Whatever method they decided to use, it seems to be one that gives most attention to the magnitude and location of the maximum horse power output, and little consideration to the resonance peaks before it.[5] The 1956 power curve represents an almost perfect parabola, with a perfectly smooth ramp up starting at 2000rpm and peaking at 6500 rpm.

---

[5] This analysis would make sense when advertising an engine, as resonance peaks are dependent on the lengths of manifolds and the presence of resonators, which often times are varied from model to model or are effected using aftermarket products.

While the profile of the 1956 curve seems to be highly idealized and unlikely rigorously measured, the peak power output is quite accurate, matching the peak power output measured on the dynamometer and matching the rpm of peak power calculated from the numerical curve. It's also quite possible that the 1956 curve very accurately represents the power curve of an engine with a very short exhaust, as will be discussed in the next section. Shorter exhausts correspond to a slightly higher peak power output as well as a flatter torque curve and smoother power curve. The smoother curves are a result of a lack of amplification of resonance peaks, due to the lack of a resonator in the case of a short exhaust or no exhaust. The next section will explore this fact, both to give validity to the 1956 power curve (with likely a short exhaust?) as well as to give validity to our measured curve (and modeled curve) which has greater amplification of resonance peaks and was taken from the same 1956 engine with a long exhaust.

Chapter 5: Engine tuning via exhaust and intake manifold length variations

Theoretical Framework

The torque generated by an internal combustion engine is directly proportional to its volumetric efficiency, which is dependent upon, among other things, quasi-static engine characteristics such as viscous losses and charge heating.[xii] It is also dependent on the ability of the ducting system to mobilize a large mass of the fuel-air mixture from the intake valve into the cylinder and out through the exhaust valve. A "large mass of fuel-air" can be quantified using a ratio which compares the volume of fuel/air aspirated into the cylinder and the volumetric capacity of the cylinder. The volumetric efficiency of an engine varies directly with this ratio.[xiii]

Acoustic resonance of the intake and exhaust manifold can have a large effect on the ability of the ducts to move large quantities of fuel and air into the cylinder, in the case of the intake stroke, and remove combustion products from the cylinder, in the case of the exhaust stroke. To better understand how this works, it is helpful to relate the natural frequency of a fluid system to a more familiar physical system like a spring, which also contains natural frequencies. Figure
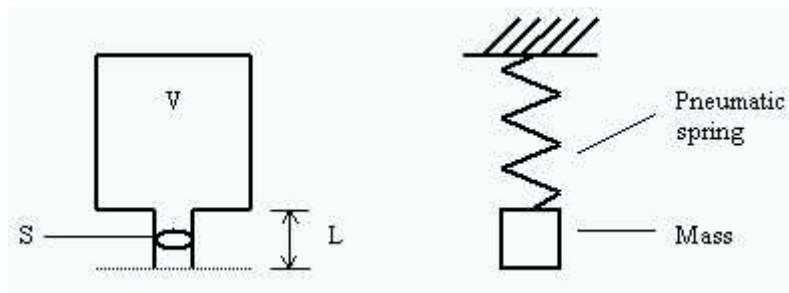
Figure 28: Helmholtz resonator system. S is the surface area of the resonator opening, L is the length of the throat, and V the volume of the cavity. Photo borrowed from Bortoluzzi

28 shows an example of an acoustic resonator, as well as conveys its spring-mass analogue. A Helmholtz resonator is constituted by a cavity and a short duct, which connects it to its fluid system.[xiv] Its behavior mirrors that of a spring-mass system, with the spring being analogous to the cavity, and the mass being analogous to the gas inside the short duct. The result is that the Helmholtz resonator system has a fundamental natural frequency of pressure oscillations which can be calculated using the following equation[xv]

$$f_{H} = \frac{c}{2\pi}\sqrt{\frac{S}{LV}}$$

(EQ 2)

Where c is the speed of sound, and S, L, and V are all defined in Figure 28. What this equation describes is that there exists discrete frequencies which a spring-mass system or an air-cavity system can be driven at which will constructively enhance the system's oscillations. By the same equation, there also exists a set of discrete frequencies which the system can be driven which

will deconstructively interfere with the system's natural frequencies, and thus dampen or inhibit the oscillations of a system. In an engine, the rotation of the piston is the mechanism driving the engine's frequency, and the intake and exhaust manifolds are the acoustic resonators reacting to the driver. Because acoustic resonance can both constructively and deconstructively interfere with fuel-air aspiration, manifold shapes and lengths are important design considerations in the process of designing both high performance engines as well as every day, efficient engines.

IC Engine Tuning

The goal in the acoustic design of an IC engine is to optimize the mass flow of fuel-air into the cylinder on the intake stroke and to remove the maximum amount of air-combustion products on the exhaust stroke. However on most engines which have fixed intake and exhaust lengths, the question really becomes, where in the rpm range can deconstructive acoustic interference be tolerated, and where on the rpm range is constructive acoustic enhancement desired? In the case of acoustic enhancement, the engine's piston is driving the intake manifold at one of its modes of natural frequency. At this point, just before the intake valve begins to open, there is a pressure wave building up on the top surface of the valve as a result of the acoustic oscillations being synced with the cylinder movement. At the moment that the valve opens, there is a pressure differential that aids the flow of air into the cylinder even more so than the cylinder vacuum could draw on its own. In the case of the exhaust stroke, constructive acoustic interference occurs when, just before the exhaust valve opens, there is a vacuum created around the opening, resulting from the air movement in the manifold shifting toward the end open to atmosphere. Upon the exhaust valve opening, the negative pressure differential aids in the
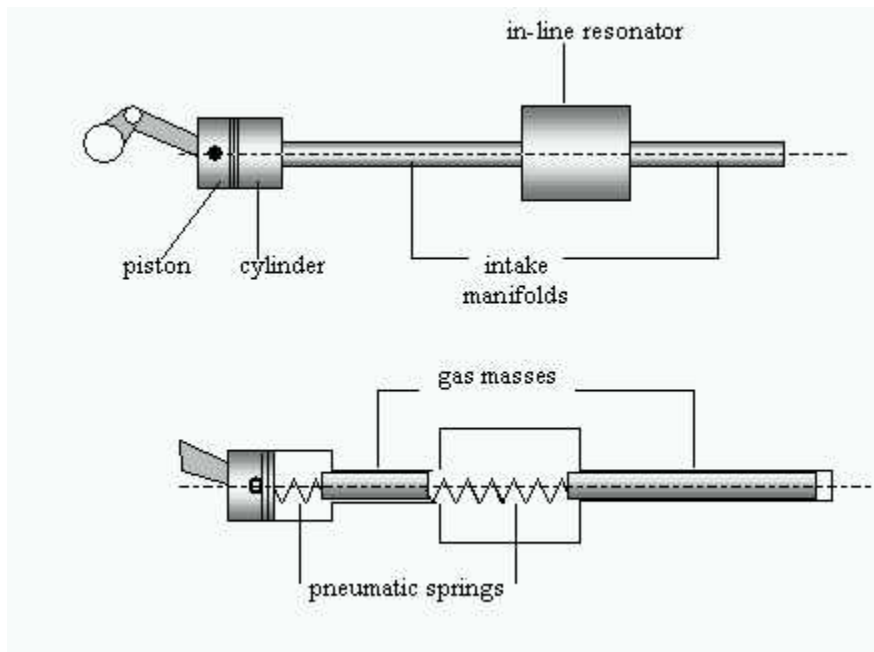

Figure 29: Acoustic resonance of a cylinder-resonator system, as explained through the mass-spring analogy. Photo borrowed from Bortoluzzi

expulsion of air and combustion products from the cylinder chamber. To visualize this process more concretely, it is again helpful to return to the mass-spring analogy of a resonating system.

Figure 29 shows the power train starting with the atmosphere, aspirated through a manifold, then through a resonator (in the absence of a resonator, the manifold itself is the resonator, at which case 'V', in EQ 1 is simply the mean volume of the pipe, and L is corrected to represent the mass of air which begins just outside the duct), and into the cylinder where the piston pushes on the flywheel, (the flywheel being the driver in this oscillating system). Figure 25 superimposes two springs over the cylinder and the resonator, which represent the natural frequencies of each (the cylinder's frequency simply being engine rpm). This system consists of two springs and two masses (the second mass being the column of air in the manifold). It is easy to picture that when these two springs are oscillating out of phase of one another, their periods are only occasionally synchronized and in some cases could be 180 degrees out of phase (deconstructive interference). However this picture also helps to visualize the harmony and amplification that is achieved when both springs are oscillating at the same rate and in the same phase. Because of the dynamic nature of engine rpm, the frequency of oscillations of the piston is not a design consideration. However intake and exhaust manifold length is static and determined by design, and can therefore be chosen such that their natural frequencies provide constructive acoustic aspiration facilitation at desired rpm values. This is the art of engine tuning.

It is apparent from EQ 2 that longer pipes have lower natural frequencies than shorter pipes. For many reasons, intake manifolds are usually much shorter than exhaust manifolds. One reason for not wanting to lengthen the intake runner too much is to minimize fuel condensation on the manifold walls during cold starting - resulting in a lean combustion or possibly no combustion at all. Exhaust manifolds tend to be longer in order to funnel the hot exhaust away from the engine as well as to provide room for a catalytic converter to reduce pollutant combustion products into harmless ones. It is therefore common to expect the exhaust length have a greater effect on the performance of the engine at lower rpms and very little at high rpms, while the design of the intake manifold length often plays a much greater effect on engine performance at high rpms rather than low.

Numerical Results

In order to bring validity to the empirical, numerical, and 1956 Triumph torque and power curves from Chapter 4, as well as to offer insight into future empirical studies involving manifold lengths, a numerical study was executed to gain insight into the causes of resonance peaks. The Virtual4Stroke engine modeling software was used to perform the study, utilizing the updated version of Brauser's engine model as a base engine, and carrying out iterative tests with the only modified parameter being the length of the exhaust (or intake). The exhaust length was varied between 1mm and 325mm at increments of 25mm. The curves are shown in Figure 30.
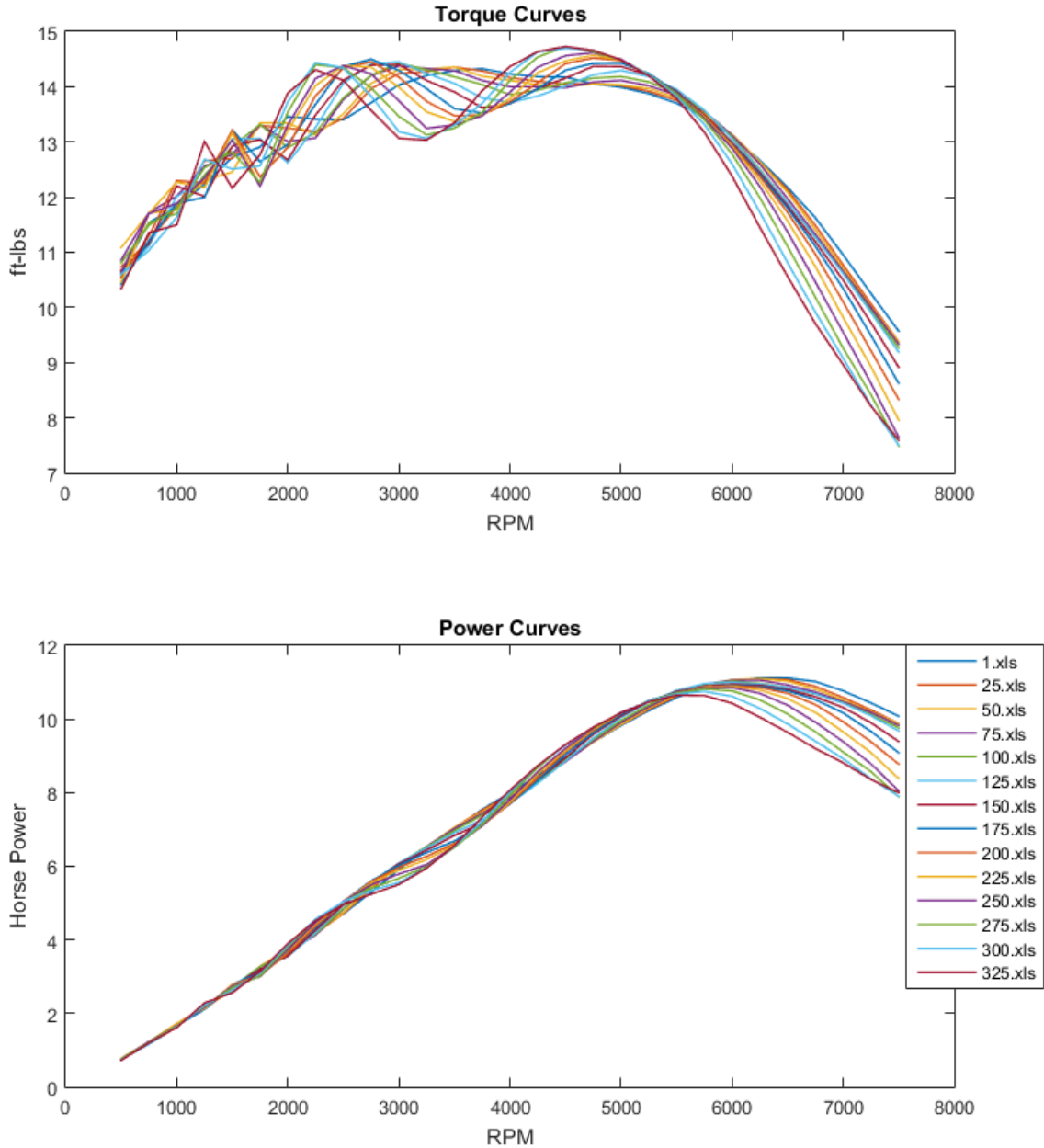
Figure 30: Effects on Torque and Power from varying exhaust manifold length

One effect that the exhaust length has on engine performance is in the magnitude and location of maximum power generation. Looking at the power curve in Figure 30, it can be seen that the 1mm exhaust produces the most horsepower and occurs at the highest rpm. Likewise the 325mm exhaust produces the lowest maximum horsepower and at the lowest rpm. This is why some bikers choose to take off their mufflers; because, along with the additional noise associated with a removed muffler so that everyone knows when you're coming, a shorter exhaust is known to

increase your power output capability. Figure 30 suggests however that this effect is more placebo than anything else. The change in horsepower associated with the exhaust length doesn't come into play until maximum rpm ranges where the curves start to deviate. So unless you are consistently getting your bike to 6000rpms, there really isn't any noticeable difference in power. The shortest exhaust also results in the lowest maximum torque generation, as can be seen in Figure 31. Not just this, but the shortest exhaust also corresponds with the "flattest" overall torque curve, providing very small if any resonance peaks throughout the rpm range due to lack of acoustic amplification. Therefore the tradeoff between taking the muffler off your bike is that you may gain marginal horse power at high rpm but will compromise torque at more traditional rpms. Figures 31 and 32 quantify the effect that a varying exhaust manifold length has on maximum torque and power generation.
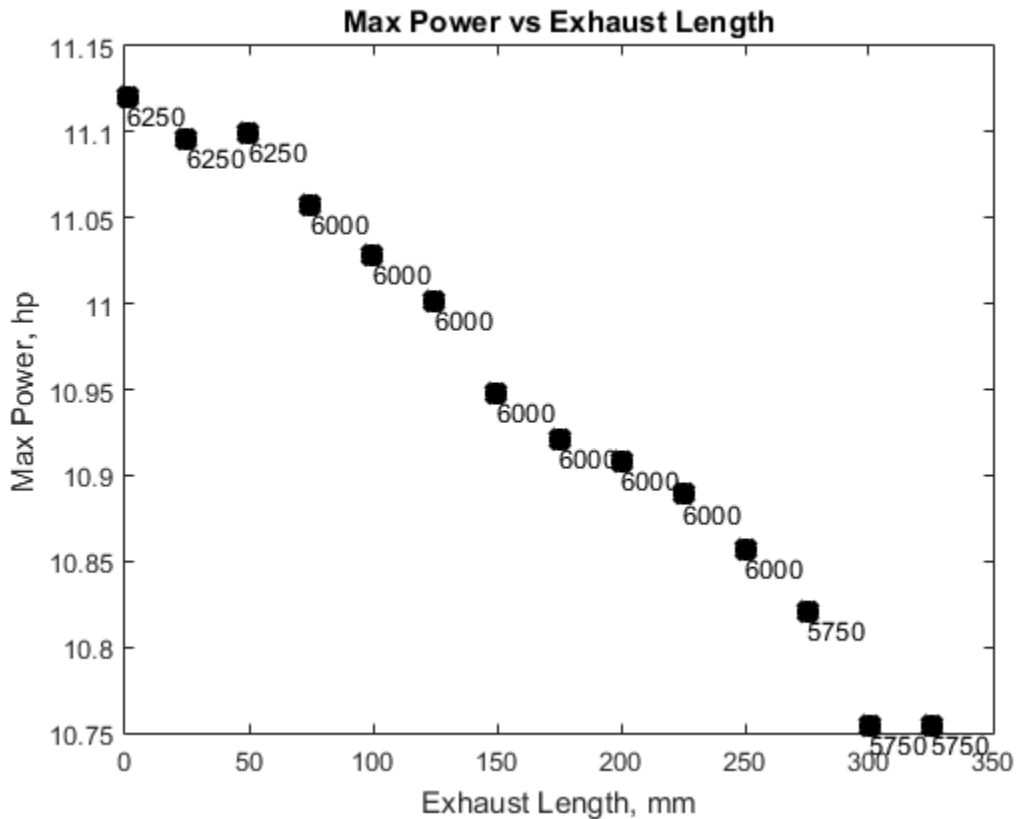
Figure 31: Max power plotted against exhaust length in millimeters. Location (rpm) of max power generation is shown next to each data point. As opposed to Figure 32, shortening the exhaust corresponds to an increase in maximum horsepower capability.
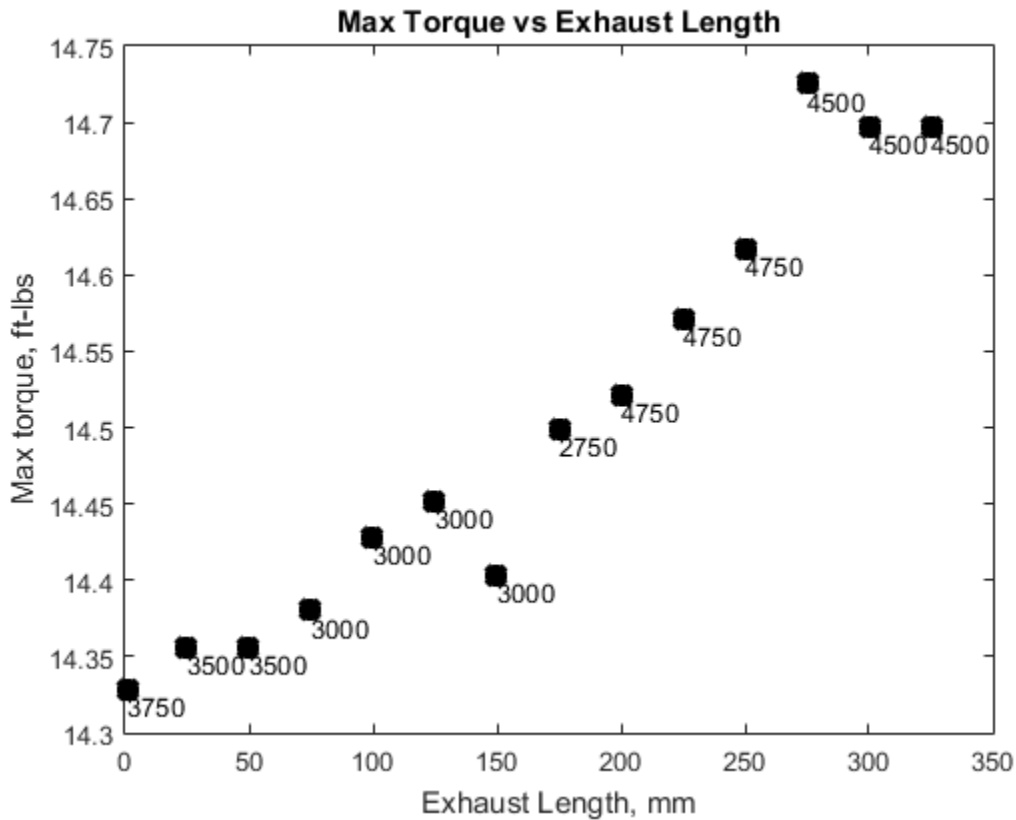
Figure 32: Max torque plotted against exhaust length in millimeters. Location (rpm) of max torque generation is shown next to each data point. While lengthening the exhaust results in a noticeable (albeit small) increasing trend in maximum torque, the data trend that is most notable is how the location of maximum torque (compared to power) changes quite drastically with exhaust length. This fact results from location of resonance peaks being directly correlated to exhaust length and the fact that torque curves are always much flatter than power curves to begin with.

While the exhaust manifold length has a slight effect on the magnitude and location of maximum horsepower generation, its most considerable effect is on maximum torque generation. To more clearly see the effects of exhaust length on torque generation, Figure 33 is presented as a less cluttered version of Figure 30.

Exhaust Length Analysis
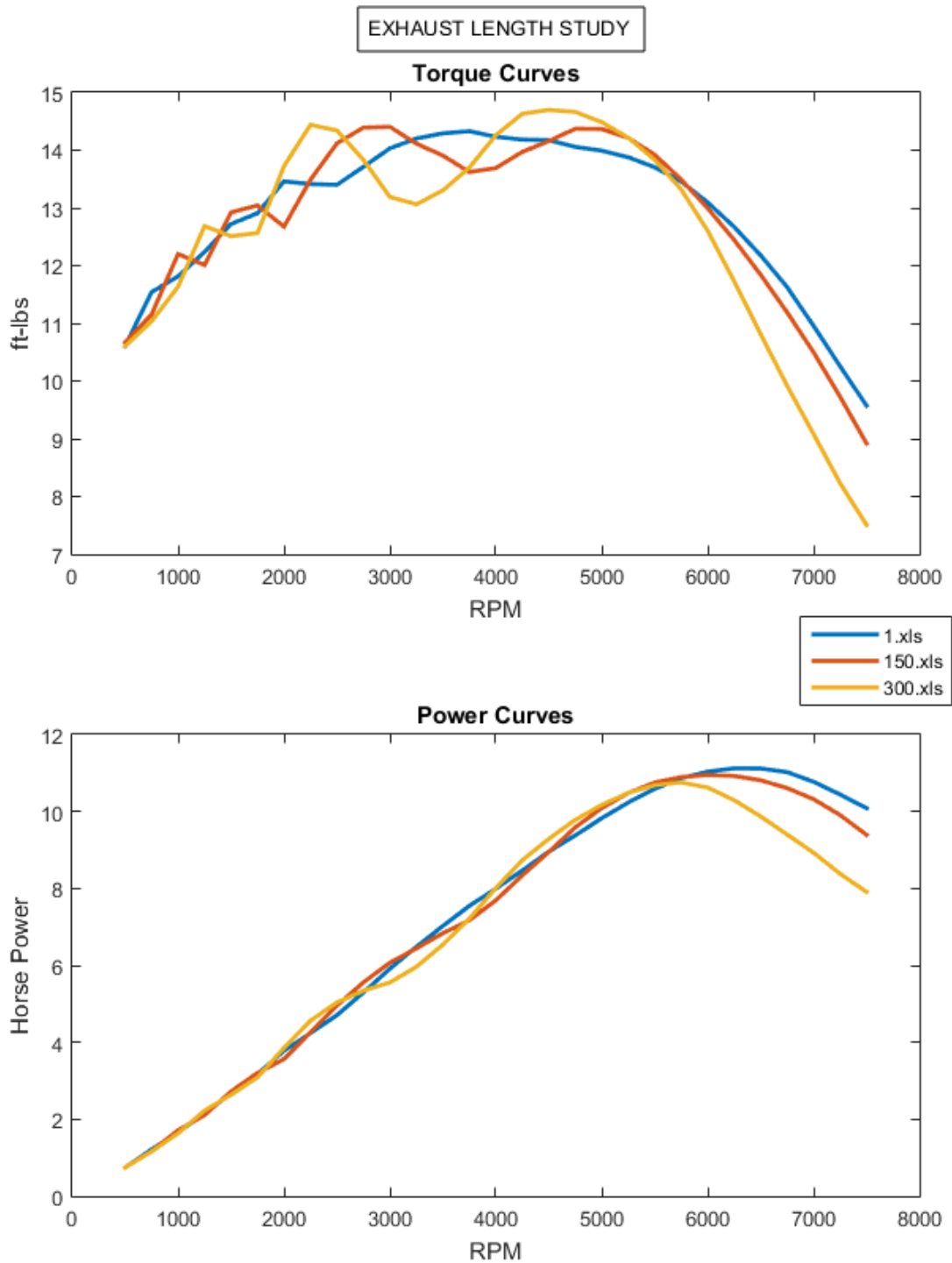
Figure 33: Lengthening the exhaust accentuates the resonance effects at low rpm while simultaneously moving the torque and power peaks to lower rpms.

As can be seen from Figure 33, a short exhaust causes a flatter overall torque curve, corresponding to a steadier rise in power. Conversely, the longer the exhaust manifold becomes, the more accentuated the resonance peaks and the lower the rpm they occur at. The bigger peaks are due to a greater column of air acting as a vacuum around the exhaust valve during the exhaust stroke. The decreasing rpm values that the peaks correspond to the decreasing natural frequencies of the increasing length pipe. The exhaust length also determines the number of torque peaks in the rpm range. The 150mm exhaust generates four torque peaks while the 300mm exhaust generates three, albeit slightly larger peaks. Design decisions, such as choosing an exhaust length, therefore can become very practical when deciding where additional torque is desired, how much, and how often.

Intake Length Results and Analysis

Varying the length of the intake manifold is a bit trickier to do in practice because it involves more physical limitations. There really isn't a restriction for making the intake runner too short, but there are for making it too long. For one, the carburetor is a part of the intake manifold and is responsible for delivering the fuel and air to the combustion cylinder. Making the intake runner too long therefore can result in excess condensation of fuel onto the manifold walls during cold starting which can result in extremely lean burn during combustion or no combustion at all. However while the design domain for the intake manifold length is more confined, it is still useful to see the effects that it has on engine performance. The results of this study are shown in figure 34. As can be expected from the higher natural frequencies resulting from the shorter intake manifolds compared to the exhaust manifolds, the intake length only effects engine performance at higher rpms (compared to exhaust effects). Increasing the intake length has no effect on the first two resonance peaks at 1500 and 2500 rpm, but does start to have an effect on the third peak at 5000 - 6000 rpm. The effect there is an increased torque and power peak corresponding with an increasing intake length. This is due to a larger column of air creating more pressure on the intake valve during the intake stroke which causes greater aspiration than ambient air alone provides.
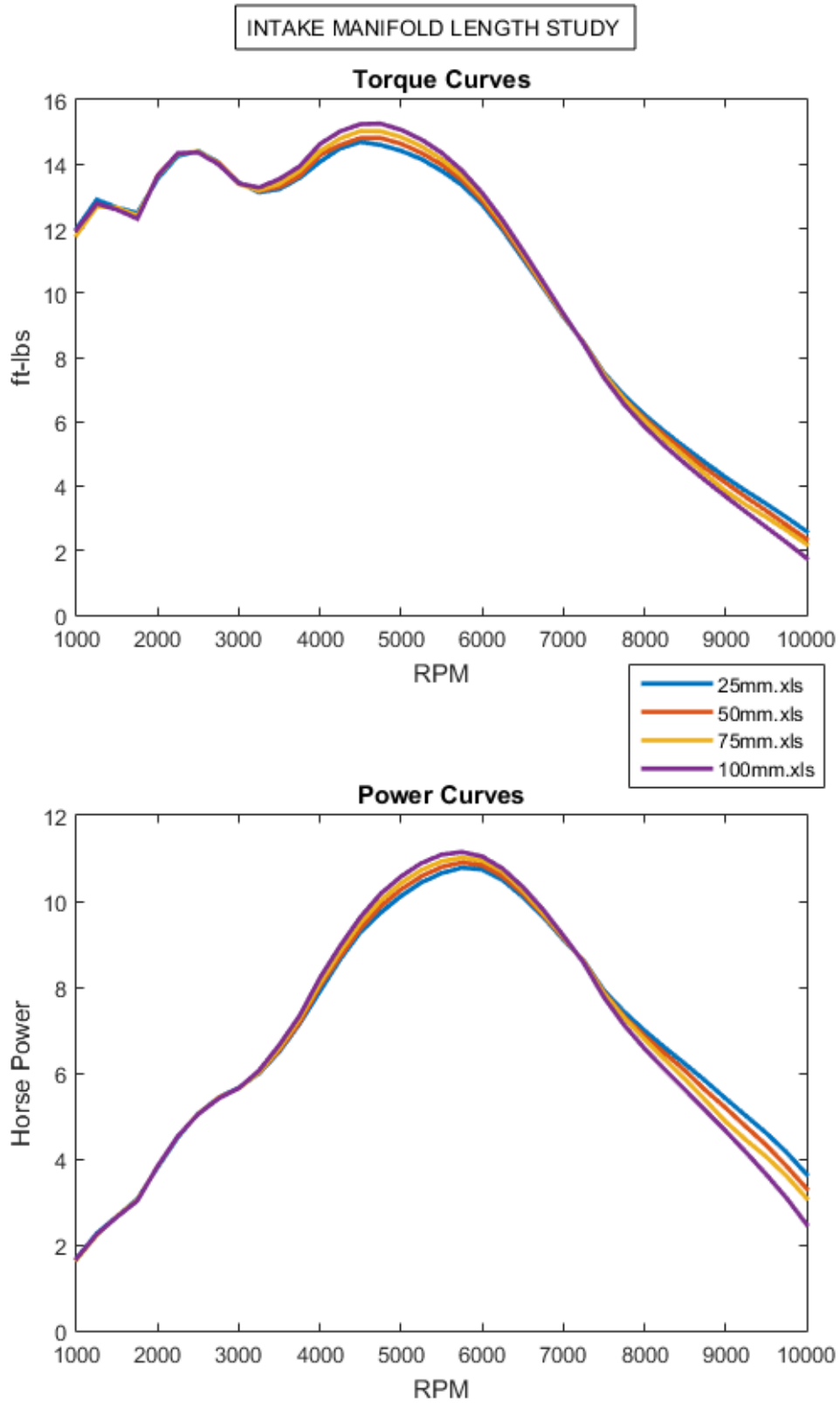
Figure 34: The effect of intake manifold length on engine performance

Chapter 6: Summary and Conclusions

Figure 27 presents three power curves representing a 1956, single cylinder, 200cc Triumph motorcycle engine which either have their source in an empirical test, numerical simulation, or a 1956 manual publication. The remarkable agreement of those three curves serves to verify each other. As a result, greater fidelity can be entrusted to the 1956 Triumph published data, the capability and intricacy of the Virtual4Stroke engine modeling software, and as well as the capability of the MAE engine dyno to record accurate engine data. Simultaneously, the differences that do result between the 1956 curve and the two curves generated from the engine this year were both qualitatively and quantitatively examined using a Virtual4Stroke study on intake and exhaust manifold length. The results of this investigation reveal that easily adjusted design features of the engine such as intake manifold length and exhaust manifold length as well as the possible addition of other aftermarket resonators are the foremost contributors to the existence, magnitude, and location of acoustic amplification of resonance peaks in the engine's torque curve. In the likely event that an engine manufacturer would not want to advertise engine capabilities that can be easily changed by the owner, the 1956 curve appears to be a curve that was generated by an engine with no exhaust pipe (a curve that represents the engine only, not aftermarket products). This claim was given evidence during Chapter 5 where numerical studies show that shorter exhaust pipes correspond to highest peak horsepower outputs occurring at highest rpms, as well as corresponding to flattest torque curves and smoothest power curves. All such characteristics are observed in the 1956 curve when compared to the numerical and empirical curves produced in 2015 with a 695mm exhaust. Additionally, all observed effects from the numerical study involving longer exhaust pipes were recreated in the empirical curve and reproduced by the software with matching magnitudes and locations of resonance peaks.

Proposed Future Research

The implications of these findings are ones that beg for further empirical data to commence. Further empirical studies on the engine dyno with varying length exhaust manifolds that match up to their equivalent engine model in Virtual4Stroke would further prove the fidelity of the engine dynamometer and DAQ equipment, as well as further validate the Virtual4Stroke software. In such an event, the engine dyno would be capable of measuring power output effects from any modifications to any engine. Some avenues available for research that are on the horizon for this laboratory include but are certainly not limited to:

- Exhaust manifold length study quantifying the effect of aspiration enhancement in an IC engine.
- In-cylinder pressure data. The equipment for this measurement is already available in the lab; only needs to be installed and wired. In cylinder pressure data, along with crank angle gathered from a manually installed optical encoder, can be used to directly measure torque as generated in the cylinder. This data together with the data measured on the dyno, can be used to quantify the losses that incur throughout the dyno power train between the piston and the dyno sprocket. This can be repeated for every engine gear to determine how gear effects engine efficiency. This information can also be used to do a study determining how chain tension

effects work losses in the power train which will be necessary to know before doing more sensitive engine studies.

- Spark advance profile modification. The distributor of the Triumph motorcycle engines is purely mechanical and 100% modifiable. A study on the effects of spark advance on torque curves would be a very informative study and provides space for an optimized spark advance profile to be pursued.
- Transferring the gasoline from a fuel cell to a graduated cylinder would allow for quantification of fuel burn and open the door for brake specific fuel consumption research.
- A CO_2 or NO_x sensor at the exhaust output combined with control of AFR, either through fuel injection or through carburetor adjustment, is the beginning of an environmental research rout that the dyno can be good for.

Proposed Methods for Future Data Acquisition Improvement

The quality of data presented in this paper was tremendously improved through the strategic design of post-acquisition filters proving the effectiveness of the data acquisition system even in the presence of large vibrations. For more sensitive engine research however, data filters become increasingly less acceptable. Future effort should be taken to build upon past efforts to further improve the signal quality from the load cell and variable reluctance sensor. Revisit the end of Chapter 2 to see a log of past successful and unsuccessful attempts to reduce signal noise for use as a starting point. Some additional recommendations to improve the lab and signal quality are listed here:

- Closed loop control of engine-dyno system is desirable and absolutely necessary for possible future research. A throttle controller should be designed using a DC motor or stepper motor to control the length of throttle cable displaced. It should be able to hold a constant position in the presence of external disturbances and vibrations, as well as control opening and closing rates. The voltage feeding the control model for the throttle controller, combined with the voltage feeding the PAU can be used to create full closed loop control of the system in order to have control over ramp rates, engine speed, and measured torque.
- To reduce signal noise and lessen the need for a post-acquisition data filter, try using the generated rpm square wave as an external clock for the LabView program to generate sample size, thus always averaging the data at an appropriate rate.
- Additional effort should be put into syncing the LabView acquisition loops which control rpm acquisition and load cell acquisition. The slowest loop will always dominate sample rate.
- To further reduce signal noise, investigate dampening material that can be put underneath both the engine stand and the dyno in order to limit the vibrations that are translated through the ground. Because the system is a dynamic system, there is not a singular damping constant that can critically damp all vibrations at every rpm. However the proper material will likely partially damp vibrations at all rpm values.

Appendix A: Virtual 4 Stroke Operation Manual

- Start the computer and login using the user *Virtual4Stroke.*
  - From the Desktop, open the shortcut titled *Design Explorer*
    - The *Design Explorer* window is organized in a design tree where user projects, engines, test procedures, and simulations are created and stored.
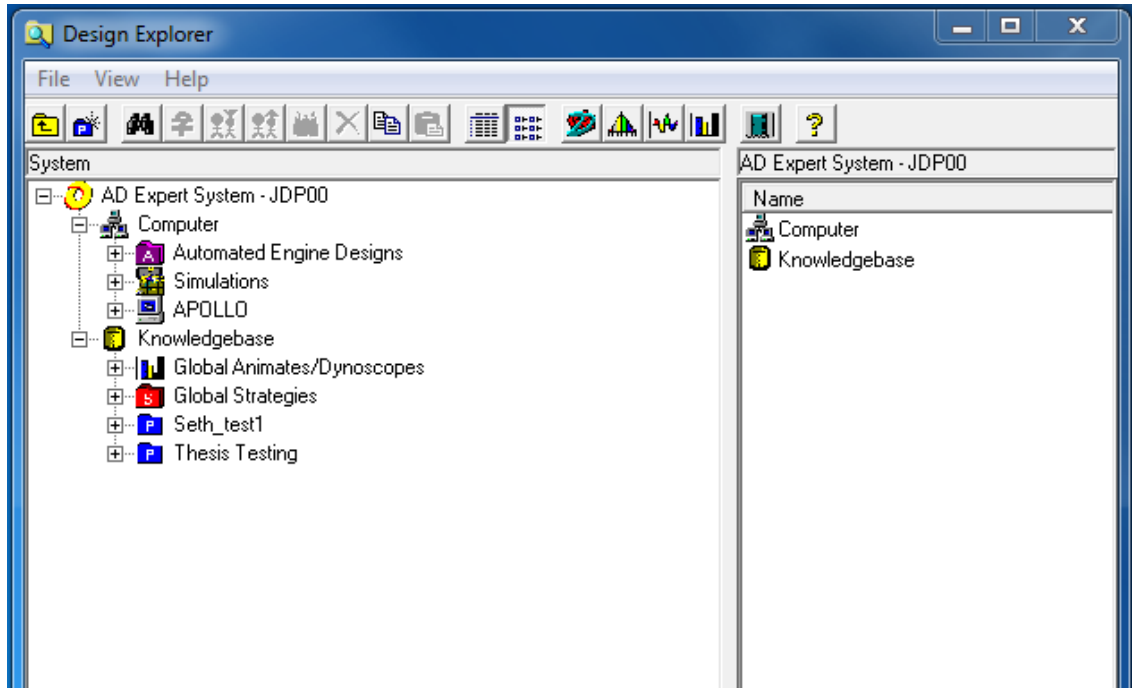
- To create a new project
  - Click on the blue project folder underneath 'File' and 'View'
  - In the 'Create New Project' dialogue box, type the name of the new project and click 'OK'.
  - A new blue 'P' folder will appear under the Knowledgebase tab in the Design Explorer with your new project name. Double click on your new project folder to view the components of your new project that are ready to be created.
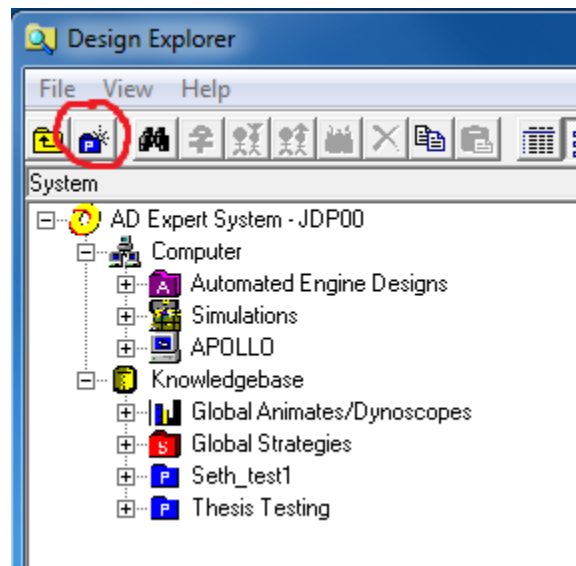
- To create a new engine
    - Right click on the green 'E' Folder under the project folder, and click on 'New Engine'.
      This opens the *Automated Design* program, which can also be opened directly from the

desktop. The window is shown at left. The window is made up of a task bar at the top, a *flow diagram* in the upper right where the engine model is laid out, a *diagnostics* window below which specifies any model errors which must be corrected before running simulations, and a *Tree View of Engine Design* at the left where engine parameters as well as simulation details are specified.
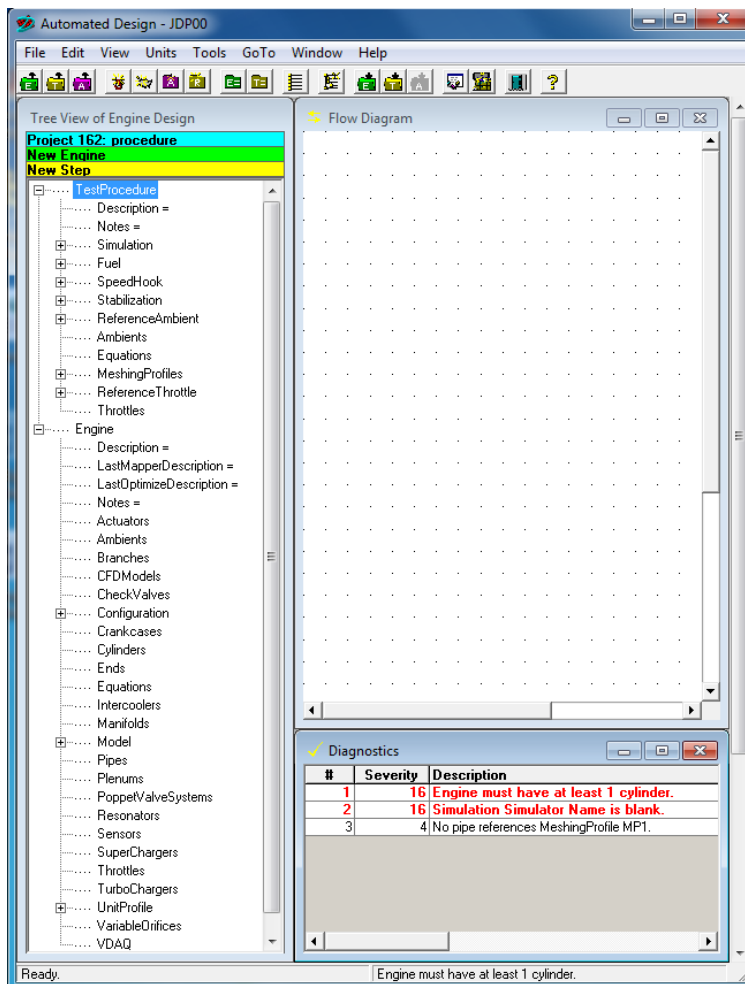
Cylinder: CYL1

Tabs: Cylinder | Friction | Head | ClosedCycle | HR/MFB | PistonMotion | Piston | Scavengings

Dimensions

Name	Value		Units
Bore	56.0	=	mm
Head surface factor	1.5000		
Heat transfer multiplier	1.0000		
Clearance volume	48.65		cc
Swept volume	#N/A		cc
Trapped compression ratio	#N/A		

Rows marked #N/A are unavailable until a crankcase is connected

Cylinder Temperature

Name	Value		Units
Liner temperature	150.0	▦ ▾	deg C
Head temperature	300.0		deg C

Close

- **To create a cylinder**
    - The user interface built into *Automated Design* is very user friendly. In the left window entitled *Tree View of Engine Design,* the two main components are 'TestProcedure' and 'Engine'. Expanding either section will reveal all of the possible available components for editing and inclusion in the engine model. The mechanics for creating an engine are simple. Right click on any engine component and choose 'New [component]' to create that component. For starters, create a new cylinder. Right click on 'Cylinders' under the Engine tree and click on 'New Cylinder'. A window entitled 'Cylinder: CYL1' will appear in which you can specify all known characteristics of the engine cylinder in which you desire to model. Click through the various tabs to edit the appropriate parameters (2 stroke or 4 stroke is specified under the 'Friction' tab). Alternatively the engine parameters can be viewed and edited by expanding the newly created cylinder in the tree view and clicking on the appropriate parameters. When completed editing the cylinder parameters, click 'Close' at the bottom of the window. To add the newly designed component to the flow diagram, simply click and hold the component icon in the tree view window and drag it onto the Flow Diagram.
    - The first engine part that should be added to the flow diagram is the 'Cylinder'. This is where the engine can be specified as a two stroke or four stroke engine, which will be necessary for the software to know before creating other engine parts. It is then good practice to build the engine model out from the cylinder in each direction, rather than building from left to right.
- **To create a valve**
    - Expand the 'Engine' section in the Tree view and right click on 'PoppetValveSystems'.

- Click 'New Poppet valve system'.
- Specify Intake or Exhaust valve
- Click 'Add…' in the upper right hand corner to design the valve. Specify as many known valve parameters of the engine that is being modeled. Click through the tabs to complete the data input. When finished, click 'OK'.
- In the 'PoppetValveSystem: PVS1' dialogue box, click close. The valve has been created.
- Click on the valve icon in the Tree View and drag it into the flow diagram.
- CAVEAT: Intake valves must be preceded by a pipe. Likewise exhaust valves must be appended by a pipe before the model reaches the ambient.
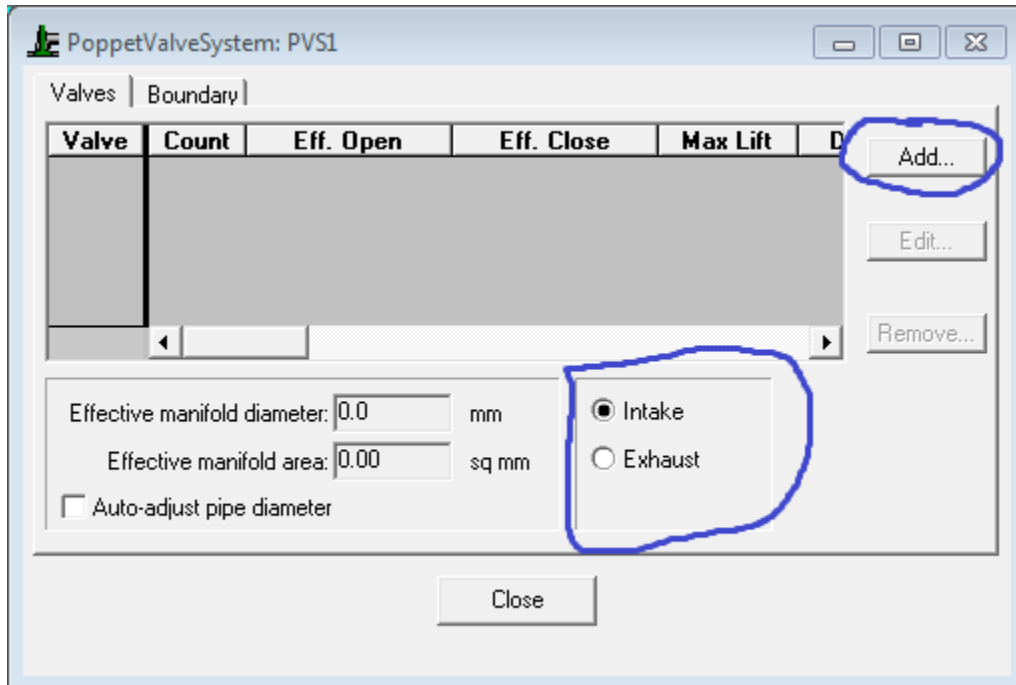
- **To create a pipe**
  - Expand the 'Engine' section in the Tree view and right click on 'Pipes'.
  - Click 'New Pipe'.
  - Specify Intake, Exhaust, or Transfer pipe under the 'Summary' Tab.
  - Under the 'Sections' tab, Click 'Add…' in the upper right hand corner to design the pipe. Pipes here are designed in sections in order to take into account non-homogenous shaped pipes. Under the 'Dimensions' tab, you can specify section length, diameters of entrance and exit, as well as bend angle and radius to fully define the profile of a pipe section. The thought is that many pipes are made out of various sections, which are pieced together in the 'Sections' tab as you continue to press 'Add…' to create each successive pipe section of the finished pipe. (Caveat: exit and entrance diameters of successive pipe sections must be equivalent. If an instantaneous change in diameter does occur, it can be modeled by inserting a pipe section of length = 0.1mm, with proper entrance and exit diameter sizes in order to couple the two different pipe diameters). Specify as many known parameters as possible. Click through the tabs to complete the data input. When finished, click 'OK'.
  - In the 'Pipe: P1' dialogue box, click close. The valve has been created.

- o Click on the Pipe icon in the Tree View and drag it into the flow diagram.
- **To create a carburetor/throttle**
  - o Expand the 'Engine' section in the Tree view and right click on 'Throttles'.
  - o Click 'New Throttle'.
  - o Leave all ratio's and multipliers at default values.
  - o In the 'CD map name' dialogue box, you may either choose to leave the Default map, or choose to import a custom one. If custom pressure to area ratio data is known, save the data as a .csv file and import the data to the CD map by choosing the 'New…' selection under the 'CD map name' dialogue box and following the onboard instructions.
  - o Click 'OK'
  - o In the 'Throttle : 'THR1' dialogue box, click close. The throttle has been created.
  - o Click on the THR1 icon in the Tree View and drag it into the flow diagram.
  - o CAVEAT: carburetors/throttles must be modeled between two pipes, namely the throttle body and the intake runner
- Follow the above mechanics to create two ambients (all engine models must start and end with an ambient which defines air properties of the operating location).

- **To make connections to the flow diagram**
  - o Right click in the 'Flow Diagram' window. The window that appears allows you to toggle back and forth between different cursor actions. Select 'make connections' and draw arrows from one engine part to the next in the proper order.

- **To create a Test Procedure**
  - o There are two options for generating a test procedure in the *Automated Design* window.
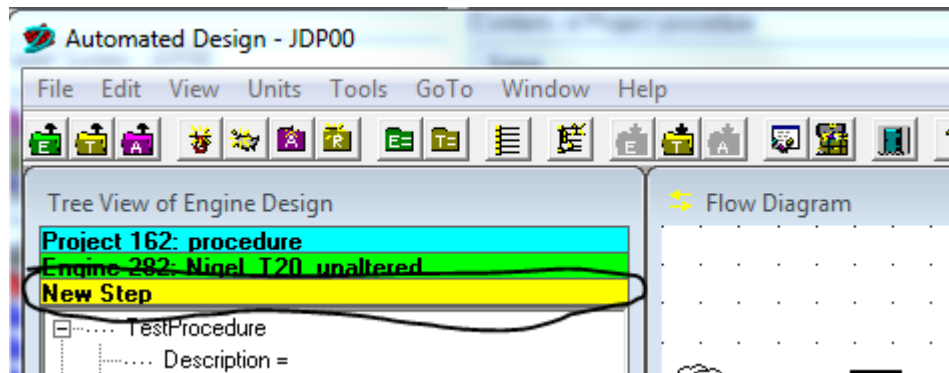
  - o The first option is to import a previously defined test procedure, which can be done by clicking on the yellow 'New Step' ribbon in the *Automated Design* window. Here you can sort through various engine models to find test procedures that have been created for previous models. Test procedures are completely general and can be used and reused on any engine.
  - o To create a new test procedure, simply expand the selections under 'Test Procedure' in the Tree View of Engine Design section and edit the values. Save the new test procedure by clicking File – Save – Test Procedure.

- **To submit a model for testing**
  - o Once the engine model is complete and test procedure is made, save both the engine and test procedure under the File – Save ribbon. Make sure that there are no diagnostic errors with severity of over 4. If such an error exists, fix it before proceeding.
  - o To submit a study, click on the 'Submit' button in the tools ribbon to submit the study to the solver.
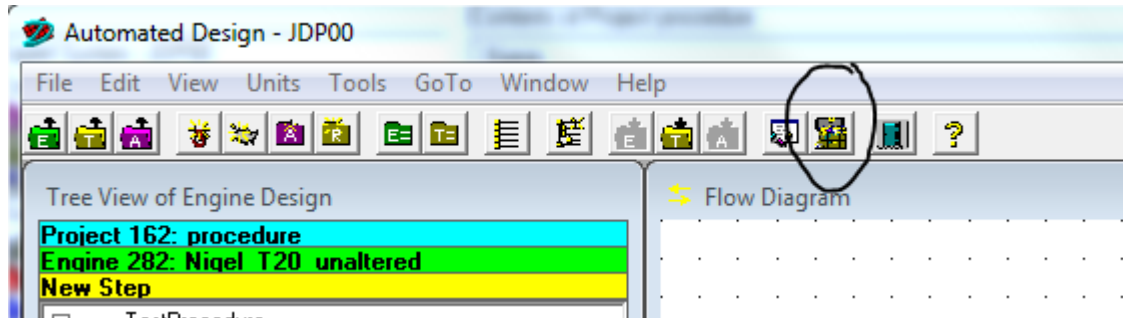
  - o Once the study is successfully submitted, return to the *Design Explorer* window.
  - o In the *Design Explorer* window, the left hand side under 'System' is a visual representation of the saved locations of engine files and studies. Follow 'AD Expert System – JDP00' to 'Computer' to 'Simulations' and click on the '+' sign to the left of 'Simulations'.
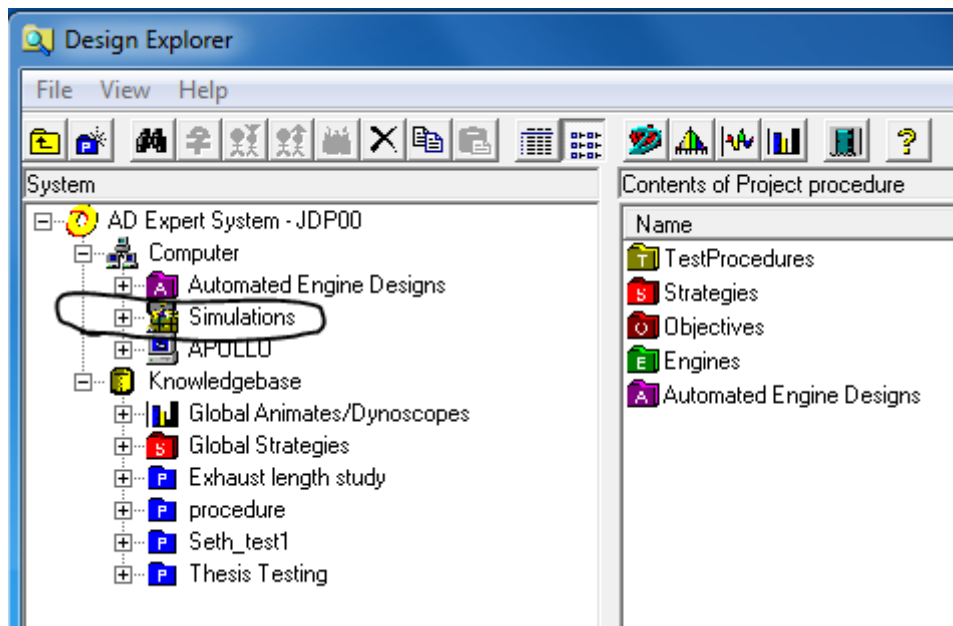
  - o Click on 'Queued' to see the study you just submitted waiting to be run. If there are no studies in 'Queued', return to *Automated Design* to resubmit your study, or click 'Refresh' under the 'View' tab to refresh the que.
  - o To move a queued study into the 'Active' section, where the solver runs the generated code, go to the start menu and click on 'Start Simulator' or type *start simulator* into the search box and select it from there. Once the simulator has been started, refresh the *Design Explorer* window by clicking 'View' – 'Refresh' and check to see that the queued study has moved to the active tab. If it has not, keep refreshing until it does.

- While the solver is running, you can view the progress of the study by right clicking on the study under the 'Active' tab and clicking 'View Progress'. From this dialogue box, the data can be exported to Excel once the study has completed.

Appendix B: Engine model parameters

Flow Diagram:
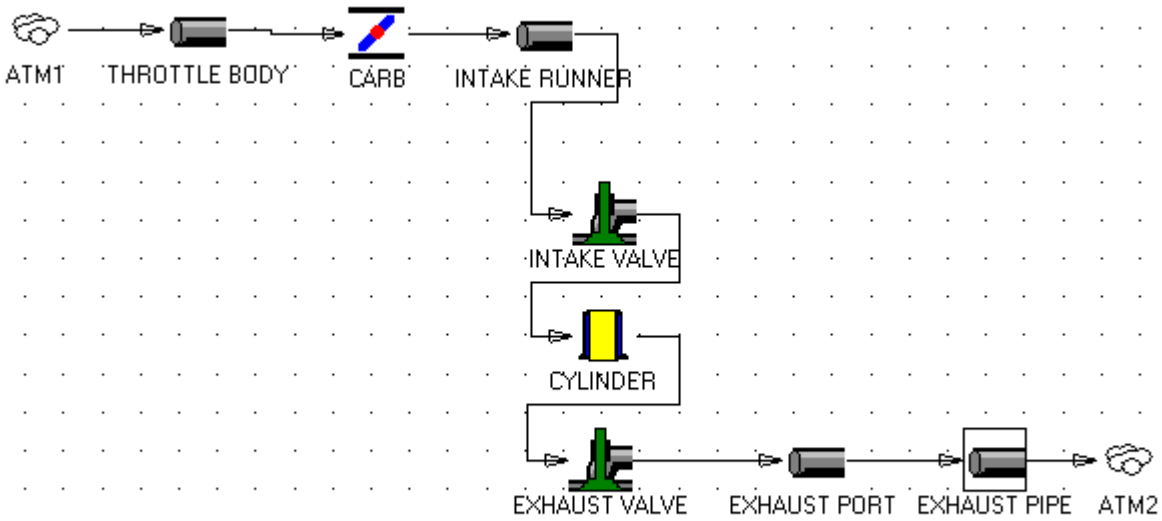
Model Parameters:

Throttle Body		
	Thickness	2 mm
	Length	49mm
	Entrance Diameter	26mm
	Exit Diameter	26mm
	Initial Gas Purity	0.2
	wall temp	20 degC
	Initial Gas Temp	20 degC
Carb	Area ratio	1
	CD map	Slide throttle
	Inflow multiplier	1
	Outflow multiplier	1
Intake Runner	Thickness	3.8 mm
	Length	111.7 mm
	Entrance Diameter	(see engine model for geometry)

	Exit Diameter	(see engine model for geometry)
	Initial Gas Purity	0.2
	wall temp	20 degC
	Initial Gas Temp	20 degC
Intake Valve	Eff. Open	25.4 deg btdc
	Eff. Close	58.95 deg abdc
	Max lift	6.5mm
	Duration	264.35 deg
	Valve type	Lift table
	Table type	Single
	Lift table	e Starting at .02
	Lift table multiplier	1
	Duration multiplier type	Complete
	Total duration multiplier	1
	valve lash	0.254
	Peg to	Open angle
	Count	1
	Stem diameter	7.8 mm
	Manifold diameter	25.1mm
	Port diameter	26.7mm
	inner seat diameter	28.4mm
	outer seat diameter	33.4mm
	Seat angle	45 deg
	model type	VEStatic
	Start RPM	1000
	End RPM	10000
	RPM increment	250
Cylinder	Bore	63mm
	Stroke	64mm
	Head Surface factor	1.32
	Heat transfer multiplier	1
	Clearance volume	33.25 cc
	Swept Volume	199.5 cc
	Compression ratio	7
	Liner Temp	150 degC
	Head Temp	300 degC
	Friction model	4 stroke SI
	Adjust for small engine	Yes
	Parasitic loss constant	0.9869 atm

	Parasitic loss factor	.0035 atm
	stroke type	4 stroke
	cylinder head type	2 valve
	Combustion model type	Single Wiebe
	Ignition timing	(see rpm table, 16 degrees maximum advance)
	Combustion efficiency	0.85
	Fueling mode	AFR
	Air-fuel ratio	12
	Equivalence ratio	0.8172
	Burn delay	10
	Burn duration	45
	Wiebe A	6
	Wiebe M	2
	Maximum MFB	1
	Mechanism type	Con-Rod
	Length	110mm
	piston height	48.6mm
	piston compression height	28.9mm
	Piston temperature	250 degC
Exhaust Valve	Eff. Open	57.7 deg bbdc
	Eff. Close	27.76 deg atdc
	Max lift	6.5mm
	Duration	265.46 deg
	Valve type	Lift table
	Table type	Single
	Lift table	e Starting at .02
	Lift table multiplier	1
	Duration multiplier type	Complete
	Total duration multiplier	1
	valve lash	0.254
	Peg to	Open angle
	Count	1
	Stem diameter	7.8 mm
	Manifold diameter	26.4mm
	Port diameter	25.2mm
	inner seat diameter	25.4mm
	outer seat diameter	28.5mm
	Seat angle	45 deg
	model type	VEStatic
	Start RPM	1000

	End RPM	10000
	RPM increment	250
Exhaust Port	Thickness	5.3 mm
	Length	55.2 mm
	Entrance Diameter	(see engine model for geometry)
	Exit Diameter	(see engine model for geometry)
	Initial Gas Purity	0.2
	wall temp	20 degC
	Initial Gas Temp	20 degC
Exhaust pipe	Thickness	4.0 mm
	Length	695 mm
	Entrance Diameter	(see engine model for geometry)
	Exit Diameter	(see engine model for geometry)
	Initial Gas Purity	0.2
	wall temp	20 degC
	Initial Gas Temp	20 degC
ATM1	Temp	20 degC
	Pressure	1 atm
	Purity	1
	Relative Humidity	50%

Appendix C: Dynamometer Operating Procedure

Dyno procedure:

1. Safety check

      a. Glasses and Ear protection for all

      b. Check for no oil and fuel leaks

      c. Oil and fuel lines not touching rotating parts or hot exhaust

      d. Electrical wires are clean and tidy

      e. Exhaust is vented properly

      f. Power supply for labview is on (switch down)

      g. No cell phones (airplane mode)

2. Power supplies for starter and brake are plugged in and ON and at ZERO amps!

3. Fuel

4. Choke is "up" = on for first minute of run time

5. Verify Engine is in proper gear (4th)

6. LabView program run, engage clutch to couple starter motor to engine

7. Ignition switch is on and battery hooked up

8. Start procedure:

      a. 1 person at throttle and ignition of engine

      b. 1 person at starter/brake/labview control

      c. Start ac starter motor, give it a hand crank towards you to help it start if necessary

      d. Once started and running adjust throttle accordingly

      e. Disengage clutch and turn off ac starter motor with the stop button on the controller!

      f. Turn off AC power supply

      g. Adjust brake power supply accordingly

9. Stop engine by either turning the ignition off, or by engaging one of the kill switches.

10. Log LabView data, done.

11. Drain Fuel

12. Disconnect battery (making sure that ignition is off)

13. Make sure everything is off and unplugged

14. Double check that everything is off and unplugged, and that fuel is cleanly drained.

Appendix D: Matlab Code:

Data filtering and processing:

```matlab
clear all
clc

%% Read in empirical data
v = .056; %volts per ft-lb v = .14; 0.0585
lcz = .74; % Load Cell zero
filepath = 'C:\Users\virtual4stroke\Pictures\Seth\Empirical
Data\second_good_run_rpm_maxed_again.xlsx';
[num,txt,raw]=xlsread(filepath);
rpm_col = 1;
torq_col = 2;

%% Read in Software data
filepath2 =
'C:\Users\virtual4stroke\Pictures\Seth\Results\Seth_T20_final_engine_step100.
xlsx';
[nums,txts,raws]=xlsread(filepath2);
rpms = nums(:,1);
rpms(isnan(rpms(:,1)),:)=[];
rpms = rpms(5:end);
rpms = add_zero(rpms);

torques = nums(:,43)*.737; % ft-lbs
torques = removeNaN(torques); %remove nans from software data
torques = add_zero(torques);

powers = nums(:,41);   % hp
powers = removeNaN(powers); %remove nans from software data
powers = add_zero(powers);


%% Remove Zeros from RPM (Empirical)
zeroind = [];
count = 0;
flagt = 0;
flagr = 0;

for i = 2:length(num)
    if num(i,rpm_col) == 0
        count = count + 1;
        zeroind(count) = i;
    end
end

index = true(1,size(num,1));
index(zeroind) = false;
num = num(index, :);

%% Data Vectors (Empirical)
gear_ratio = 2.79;
```

```matlab
rpm = num(:,rpm_col);
torque = (num(:,torq_col)-lcz)/(v*gear_ratio); %ft/lbs
power = rpm.*torque./5252;


%% Filter Length Preparation

rpm_max = max(rpm);
dx = 250;
data_count = zeros(round(rpm_max/dx),2);

for i = 1:length(data_count)
    data_count(i,2) = dx*i;
    for j = 1:length(num(:,rpm_col))
        if num(j,rpm_col) > dx*i - dx/2  &&  num(j,rpm_col) < dx*i + dx/2
            data_count(i,1) = data_count(i,1) + 1;
        end
    end
end


%% Filter Empirical Data
count = 0;
rowcount = 0;
storage = zeros(1,3); %columns: RPM,torque,power
filtered_data = zeros(1,3); %columns: rpm_mean,torque_mean,power_mean

dcount = 1;
data_count = flipud(data_count);
dx = data_count(dcount);

% Reiman Sum with a varying domain width
for i = 1:length(rpm)
    count = count+1;
    storage(count,1) = rpm(i);
    storage(count,2) = torque(i);
    storage(count,3) = power(i);

    if count == dx || i == length(rpm)
        count = 0;
        rowcount = rowcount+1;
        dcount = dcount+1;
        filtered_data(rowcount,1) = sum(storage(:,1))/dx;
        filtered_data(rowcount,2) = sum(storage(:,2))/dx;
        filtered_data(rowcount,3) = sum(storage(:,3))/dx;
        dx = data_count(dcount);
        storage = zeros(1,3);
        if dx == 0
            dcount = dcount+1;
            dx = data_count(dcount);
        end

    end
end
```

```matlab
% Apply smoothing to reiman averaging
filter_step_rf = dx;
filter_step_f = 3;
smooth_type_f = 'moving';
rpmf = filtered_data(:,1);
torquef = filtered_data(:,2);
powerf = filtered_data(:,3);
mov = smooth(rpmf,filter_step_f,smooth_type_f); % smooth generated rpm
movt = smooth(torquef,filter_step_f,smooth_type_f); % smooth generated torque
movp = smooth(powerf,filter_step_f,smooth_type_f); % smooth generated power



%% Plotting Filtered Data on top of Empirical Data

% Plot Empirical Data
subplot(2,1,1),
plot(rpm,torque,'r.');
hold on
title('Torque')
xlabel('RPM')
ylabel('Torque, ft-lbs')
hold off

subplot(2,1,2),
plot(rpm,power,'b.');
hold on
title('Power')
xlabel('RPM')
ylabel('Power, HorsePower')
hold off

% plot filtered data
subplot(2,1,1), hold on
plot(mov,movt,'k--','LineWidth',3) % plot smoothed generated torque
hold off

subplot(2,1,2), hold on
plot(mov,movp,'k--','LineWidth',3) % plot smoothed generated power

%% Plot filtered Empirical Data next to modeling software output.

figure()
subplot(2,1,1),
hold on
plot(mov,movt,'r-','LineWidth',2) % plot smoothed generated torque
plot(rpms,torques,'r--','LineWidth',2); % Software Torque
legend('Empirical Torque','Virtual4Stroke Torque');
title('Torque comparison')
xlabel('RPM')
ylabel('Ft-lbs')
hold off

subplot(2,1,2),
figure()
```

```matlab
hold on
plot(mov,movp,'b-','LineWidth',2) % plot smoothed generated power
plot(rpms,powers,'b--','LineWidth',2);  % Software Power
legend('Empirical Power','Virtual4Stroke Power','TigerCub Bible published
curve (1956)');
title('Power Comparison')
xlabel('RPM')
ylabel('HP')
hold off


%% Torque differential comparison
figure(4)
plot(rpms(2:end),diff(torques),'g-','LineWidth',2) % software differentials
hold on
plot(mov(2:end),-diff(movt),'b-','LineWidth',2) % empirical differentials
title('Torque Derivitive Comparison')
legend('Software Output', 'Empirical Data')
xlabel('RPM')
hold off

%% Power differential Comparison
figure(5)
plot(rpms(2:end),diff(powers),'g-','LineWidth',2) % software differentials
hold on
plot(mov(2:end),-diff(movp),'b-','LineWidth',2) % empirical differentials
title('Power Derivitive Comparison')
legend('Software Output', 'Empirical Data')
xlabel('RPM')
hold off

%% Plot Signal Differentials
figure()
plot(rpm(2:end),diff(rpm),'r.');
hold on
plot(rpm(2:end),diff(torque),'b.');
legend('RPM','Torque')
title('Signal Differentials')
xlabel('RPM')
ylabel('Signal Derivitive')
hold off
```

function 'removeNaN.m'

```matlab
function [ vector_out ] = removeNaN( vector_in )
% removes NaN from a numeric array

rpms = vector_in;
rpms(isnan(rpms(:,1)),:)=[];
vector_out = rpms(5:end);


end
```
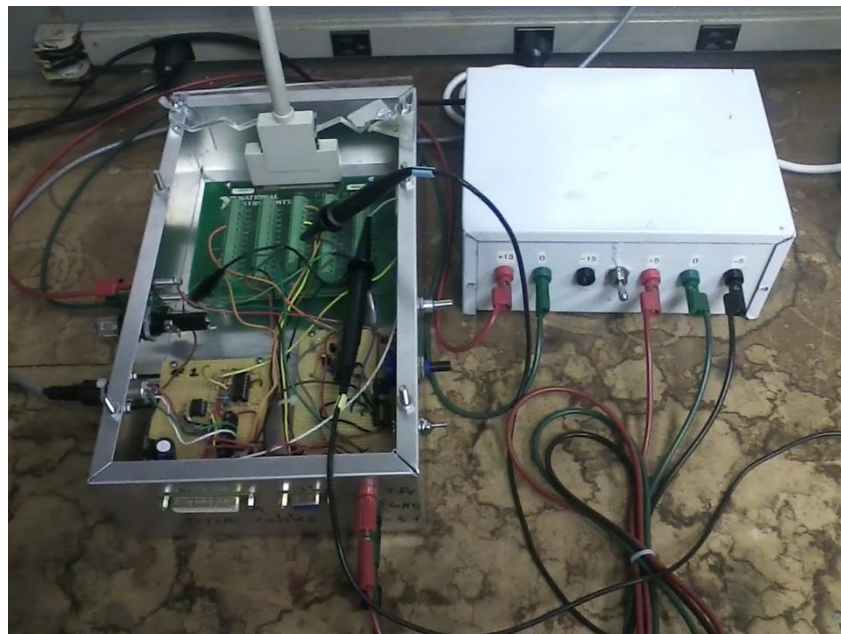
function 'add_zero.m'

```matlab
function [ vector_out ] = add_zero( vector )

vector_out = zeros(length(vector)+1,1);
vector_out(2:end) = vector;

end
```

Appendix E: Laboratory Development

Figure 35: DAQ system. National Instruments Analogue/Digital IO card.
Custom built circuit boards: Low pass filter, Digital to Analogue convertor
for RPM signal, frequency to voltage converter.

Figure 36: Custom built power supply and voltage regulator from an online kit.
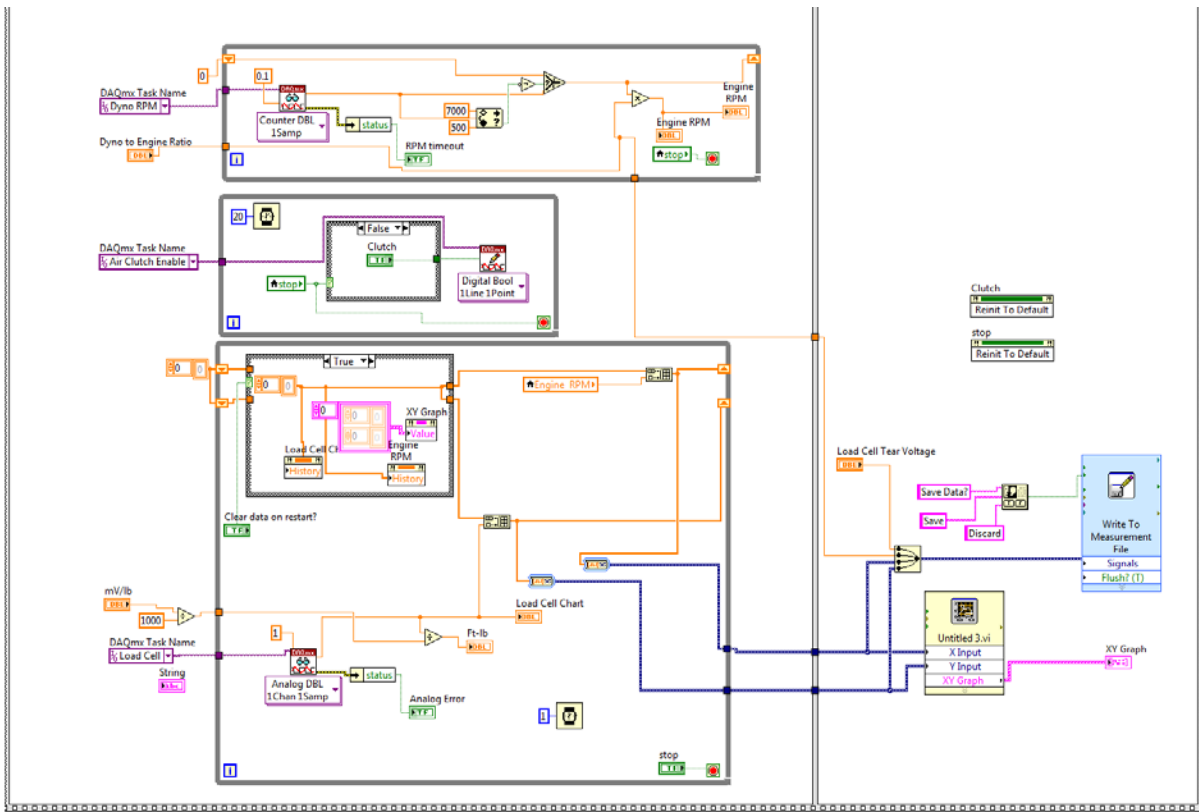*Compact and accurate. Used to power the DAQ system.*
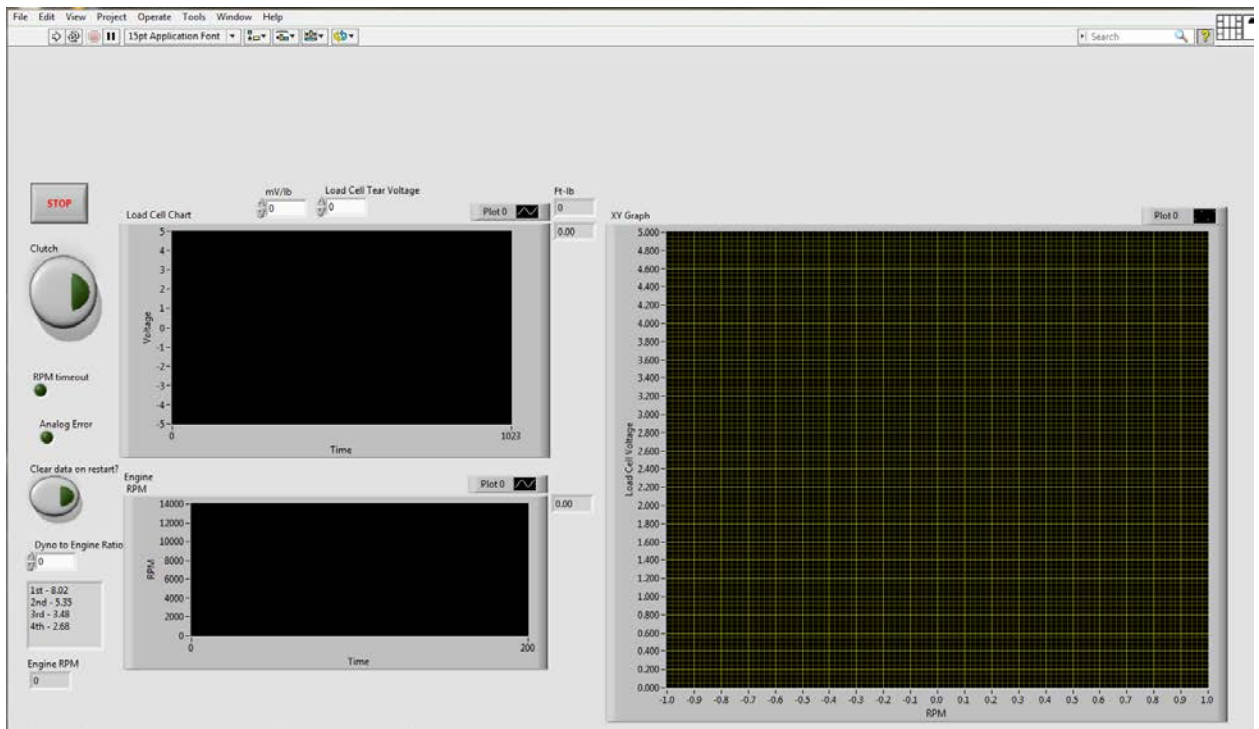
Figure 37: Labview Block diagram (above) and front panel (below) used to process data from DAQ card. Developed under the direction of Jon Prevost
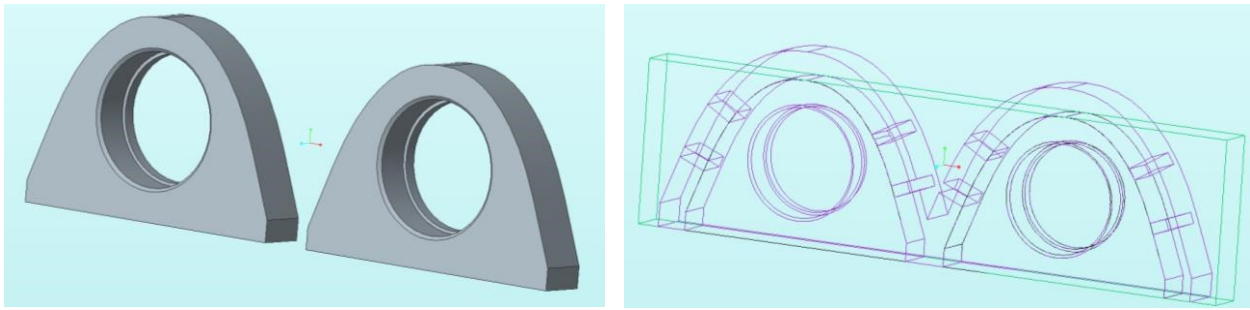
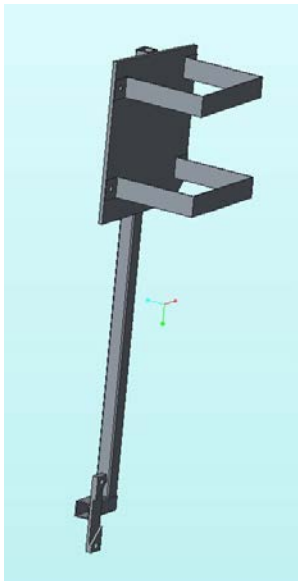*Figure 38: Axle flanges. Drawn in Creo 2.0. Coded toolpaths for CNC milling*

Figure 39: Fuel Tank mounting assembly drawn in Creo 2.0

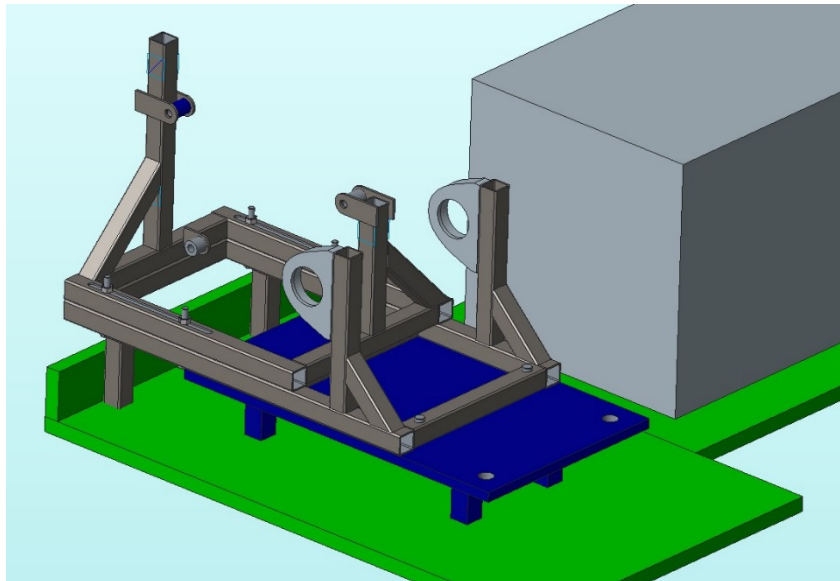*Figure 36: Triumph motor stand assembly. Drawn in Creo 2.0*

Works Cited

Bortoluzzi, Daniele. "FLUID DYNAMIC STUDY OF INTAKE MANIFOLDS OF INTERNAL

    COMBUSTION ENGINES IN PRESENCE OF ACOUSTIC RESONATORS." N.p., n.d.

    Web.

"Eastern Draft Horse Association." N.p., 18 Oct. 2010. Web.

    <http://www.easterndrafthorse.com/index.htm>.

Estall, Mike. *The Triumph Tiger Cub Bible: A Personal History of the Triumph Terrier and*

    Tiger Cub. Vol. Chapter 3. Dorchester: Veloce, 2000. Print.

"History of Dynamatic™ Corporation." *History of Dynamatic Corporation*. Dyne Systems, Inc,

    2014. Web.

Littman, Michael G. "Electrical, 1956 Terrier." *Princeton University*. Trustees of Princeton

    University © 2014, 06 Mar. 2014. Web.

Optimum Power Technology. "Virtual 4-Stroke Design and Simulation Software." Optimum,

    2015. Web.

Peters, Lauren. "Dynamometer History - A Timeline of Innovation." *Enzine @rticles*. N.p., 03

    Mar. 2008. Web.

Triumph Engineering Co. LTD. *Triumph Workshop Instruction Manual*. Publication. Vol. 8.

    N.p.: n.p., 1964. Print.

References

[i] Peters, Lauren. "Dynamometer History - A Timeline of Innovation." Enzine @rticles. N.p., 03 Mar. 2008. Web.

[ii] Ibid.

[iii] "History of Dynamatic™ Corporation." History of Dynamatic Corporation. Dyne Systems, Inc, 2014. Web.

[iv] "Eastern Draft Horse Association." N.p., 18 Oct. 2010. Web.

[v] Ibid

[vi] "Faraday's law." The Columbia Encyclopedia, 6th ed.. 2015. *Encyclopedia.com*. 4 Jan. 2016

[vii] Dwight, Herbert B.; Fink, D. G. (1949). Electromagnetic Induction of EMF in Sec. 2 - Electric and   Magnetic Circuits".

[viii] Optimum Power Technology. "Virtual 4-Stroke Design and Simulation Software." Optimum, 2015.

[ix] Littman, Michael G. "Electrical, 1956 Terrier." Princeton University. Trustees of Princeton University © 2014, 06 Mar. 2014.

[x] Triumph Engineering Co. LTD. Triumph Workshop Instruction Manual. Publication. Vol. 8.

[xi] Estall, Mike, 1956. *The Triumph Tiger Cub Bible,* Chapter 3, page 26

[xii] Bortoluzzi, Daniele.

[xiii] Ibid.

[xiv] Ibid.

[xv] Ibid.